





20456973

**LIBRARY**  
**Michigan State**  
**University**

This is to certify that the  
dissertation entitled

FREQUENCY DOMAIN ROBUST CONTROL OF DISTRIBUTED  
PARAMETER SYSTEMS

presented by

YOSSI CHAIT

has been accepted towards fulfillment  
of the requirements for

Doctor of Philosophy degree in Mechanical Engineering

*Clark Radcliffe* *Chairman* *Modell*  
Major professor

Date June 29, 1988



**RETURNING MATERIALS:**  
Place in book drop to  
remove this checkout from  
your record. FINES will  
be charged if book is  
returned after the date  
stamped below.

FEB 07 1994

1802

**FREQUENCY DOMAIN ROBUST CONTROL OF DISTRIBUTED PARAMETER SYSTEMS**

by

**YOSSI CHAIT**

**A DISSERTATION**

submitted to  
Michigan State University  
in partial fulfilment of the requirements  
for the degree of

**Doctor of Philosophy**

Department of Mechanical Engineering

1988

512-41128

## ABSTRACT

Realizable control methods for distributed parameter systems (DPS) are usually implemented using finite order controllers designed for truncated models and are subject to spillover effects. In general, it is difficult to guarantee closed-loop controlled DPS stability and performance in the presence of this spillover. This problem is solved in this dissertation. Our work allows for truncated-model-based control design for DPS in a modal representation of an infinite partial fraction expansion. A "tube of uncertainty" is obtained via bounds on the DPS model truncation error. The Nyquist plot of the actual system is shown to lie within the "tube of uncertainty" of the plot for the truncated model. This combined with a single-input single-output frequency domain stability criterion developed here is utilized to define an modified criterion where one can analyze the stability of the actual DPS. The modified criterion is employed in studying frequency domain controller designs for enhanced stability and active suppression of Bernoulli-Euler beam vibration. The limitations imposed by the structure of typical truncated models and by the truncation errors are discussed.

The theory presented here does not require a prerequisite understanding of sophisticated mathematics, provides a easy to compute robustness measure with respect to model truncation errors and parameter variations, and allows for classical frequency domain controller design. The practical design method can be utilized to decide the necessary order of the model truncation required to guarantee closed-loop frequency response performance criteria.

To my parents, Tova and Samuel,  
and to my brother, Arnon.

#### ACKNOWLEDMENT

The completion of this dissertation would have been impossible without the consideration of my two academic advisors. Dr. Clark J. Radcliffe directed me in the development of necessary skills and confidence required to meet the challenges of the future, inspired my imagination and also the courage to pursue this imagination upon which this work is based upon. To Dr. Charles R. MacCluer -- a truly inspiring teacher and counselor -- for his guidance and friendship. His seemingly unlimited capacity to sort order out of chaos have contributed immensely to the tangible results embodied in this work. I am eternally indebted to both advisors for making this work rewarding and enjoyable.

The final substance and form of this dissertation is due to the assistance of my guidance committee. My sincere thanks to Dr. Suhada Jayasuriya - a role model as a researcher in the controls area - for the many thought provoking discussions, and to Dr. Ronald Rosenberg for showing me how one can operate in an academic environment with class (also for teaching me tennis). Thanks are also extended to the other committee members Dr. Hassan Khalil and Dr. Robert Schlueter who rendered many useful suggestions for improving content and clarity.

I would like to express my gratitude to the following friends. To Susan Nordgaard for her love, understanding, and cooperation. To Jim Oliver, Ace Sannier, Andy "Party" Hull, Jackie Carlson, Steve Southward, Zbig Zalewski, and many many others for making my stay at MSU such an intellectual pleasure. Thanks are also extended to Bob

Rose for taking a personal interest in making things go smoothly for me here.

Finally, I would like to thank to persons who made all this possible financially, Dr. Eric Goodman, director of the Case Center for CAEM, and Dr. John Lloyd, chair of the ME department, both at MSU.

## TABLE OF CONTENTS

	Page
List of Figures	vii
Nomenclature	viii
§1. Introduction	1
1.1 Literature Review	1
1.2 Objectives	7
1.3 Organization of the Dissertation	8
§2. Extended Nyquist Stability Criterion for Distributed Parameter Systems	9
2.1. Extended Nyquist Stability Criterion for SISO	10
2.2 Extended Nyquist Stability Criterion for MIMO	16
§3. Frequency Domain Truncation Bounds	17
3.1. Bounds for First Order Terms	17
3.2. Bounds for Second Order Terms	19
3.3. Overall Bound	23
3.4. Bounds for Terms About Any Vertical Axis	23
3.5. Numerical Computation of the Bounds	27
3.6. Graphical Interpretation of the Error Bounds	28
3.7. Numerical Example: Error Bounds Calculation	29

	Page
§4. Frequency Domain Stability Analysis Using Truncated Models	31
4.1. Generation of Nyquist Plots	31
4.2. Closed-Loop Stability	34
4.3. Numerical Example: Stability Verification	36
§5. Control Design in the Frequency Domain	43
5.1. Design for Improved Damping and Stability Margin	43
5.2. Closed-Loop Frequency Response Shaping	50
Conclusions	58
Recommendations for Future Work	60
Appendix A: Mathematical Preliminaries	65
Appendix B: The Laplace Transform Pair	72
References	80

## LIST OF FIGURES

	Page
Fig. 2.1 The feedback control system including measurement noise	10
Fig. 3.1 The truncation bounds	23
Fig. 3.2 The modified first order root	24
Fig. 3.3 The modified second order root	27
Fig. 3.4 Bound circles and the tube of uncertainty	29
Fig. 4.1 The feedback control system including input disturbances	32
Fig. 4.2 The different stability cases of the modified Nyquist criterion: a) guaranteed stability, b) guaranteed instability, and c) undetermined stability	35
Fig. 4.3 The Bernoulli-Euler beam showing the actuator and sensor	37
Fig. 4.4 Nyquist plot for $G_c=1$ , $n=1$ , and $x_a=1/7$ $x_s=5/7$	40
Fig. 4.5 Nyquist plot for $G_c=1$ , $n=2$ , and $x_a=1/7$ $x_s=5/7$	41
Fig. 5.1 Nyquist plot for single lead, $n=2$ , and $x_a=1/7$ $x_s=5/7$	44
Fig. 5.2 Nyquist plot for single lead, $n=4$ , and $x_a=1/7$ $x_s=3/7$	47
Fig. 5.3 Local Nyquist plot of Fig. 5.2	48
Fig. 5.4 Nyquist plot for double lead, $n=4$ , and $x_a=1/7$ $x_s=3/7$	49
Fig. 5.5 Closed-loop frequency response for the system in Fig. 5.2	51
Fig. 5.6 Detailed closed-loop frequency response of the 1st mode	52
Fig. 5.7 Detailed closed-loop frequency response of the 2nd mode	53
Fig. 5.8 Detailed closed-loop frequency response of the 3rd mode	54
Fig. 5.9 1st vibration mode in Fig. 5.2 and $K=2.1$	55
Fig. 5.10 1st vibration mode in Fig. 5.4 and $K=1$	56

## NOMENCLATURE

- $C(s)$  = rational feedback compensator
- $E(s)$  = truncation error
- $G(s)$  = distributed parameter system transfer function
- $G_n(s)$  = truncated distributed parameter system transfer function
- $G_c(s)$  = rational forward compensator
- $G_f(s)$  = rational feedback compensator
- $H(s)$  = closed-loop transfer function
- $h(t)$  = closed-loop impulse response
- $P(s)$  = forward transfer function
- $Q(s)$  = open-loop transfer function
- $R$  = frequency response error magnitude bound
- $s$  =  $\sigma + j\omega$
- $t$  = time
- $\omega$  = frequency
- $\omega_k$  = mode natural frequency
- $\zeta_k$  = mode damping factor
- $\delta_k$  = modal amplitude
- $\sigma$  = location of the vertical axis in the Inverse Laplace Transform
- $L^1(\cdot, \cdot)$  = the space of absolutely integrable functions on  $(\cdot, \cdot)$
- $L^\infty(\cdot, \cdot)$  = the space of essentially bounded functions on  $(\cdot, \cdot)$
- $\|\cdot\|_1$  = the usual norm on  $L^1$
- $\|\cdot\|_\infty$  = the usual norm on  $L^\infty$
- $\inf_\omega |\cdot|$  = infimum of  $|\cdot|$  over  $\omega$
- $\sup_\omega |\cdot|$  = supremum of  $|\cdot|$  over  $\omega$
- $*$  = convolution operator

## §1. INTRODUCTION

### 1.1. Literature Review

Research in the area of linear distributed parameter systems (DPS) control has intensified in the past decade. Most of the work was motivated by the need to achieve satisfactory performance of large space structures, scheduled to be launched into space in the near future [Juang 1986]. Such structures are made of mechanical parts with small natural damping and sustain long lasting vibration due to disturbances or during maneuvers which can significantly degrade their performance. To achieve a satisfactory performance, it is necessary in many cases to implement an active controller which is closed-loop stable and performs well in the presence of this flexibility. Other contributions were motivated by similar problems arising in flexible robots, long boom antennas, manufacturing, and heating processes.

Models for DPS have an infinite number of degrees of freedom and are characterized by nonrational transfer functions in the frequency domain and a infinite-order set of matrices in the state space domain. Practical constraints require that the controller be implemented using a reduced (finite) order model (ROM) and that it should be robust with respect to parameter uncertainties. The common practice is to obtain a full-order model and then synthesize a controller using a finite-order model, truncated according to some criterion, with the objective of meeting performance specification for the full-order closed-loop system. Because of the above implementation constraints most of the contributions deal with ROM-based controllers.

Early work on DPS control [e.g. Leonhard 1953] included the first few system modes in the ROM, assuming that these modes dominate the response and that the neglected modes will not be affected by closing the loop. This branch of DPS control is now known as Modal Control, and is described in the classic control text by Takahashi (1970). Modal Control can also be applied in finite-dimensional systems [Simon 1968]. When applied to a DPS system, Modal Control cannot guarantee stable closed-loop performance for the following reason.

Most ROM-based control methods utilize both actuators and sensors. The actuator force on the neglected modes and the contribution of the neglected modes in the sensor output are referred to as control and observation spillover, respectively. It has been shown, theoretically [Balas 1978, Meirovitch 1983, Leipholz 1984, and Chait 1988d] and experimentally [Breakwell 1983, and Sundararajan 1984], that excessive spillover degrades the DPS performance and in extreme cases destabilizes the closed-loop controlled DPS. In fact, for any ROM-based control method, there is uncertainty as to whether or not the controller will have the desired effect on the actual DPS.

The infinite dimensionality of DPS models renders the well developed finite dimensional control theory unsuitable. In DPS control, one must first establish existence of finite-dimensional controllers. It was shown [Gibson 1980] that it is not always possible to stabilize a DPS with a finite-dimensional controller. Triggiani (1975) presented counter examples demonstrating that controllability of the DPS does not imply stabilizability. Similar conclusions were arrived at by Vidyasagar (1987). Roughly speaking, a finite-dimensional controller can stabilize a finite-dimensional system; the analogy in DPS is that an infinite-dimensional controller is required to arbitrarily shift an infinite number of eigenvalues. Therefore,

much of the theoretical work was initially focused on putting necessary and sufficient conditions on existence of initially infinite-dimensional and later finite-dimensional controllers for various classes of DPS. Once existence was shown, interest shifted to the development of extensions of time-domain and frequency domain finite-dimensional control methods: pole placement, optimal, adaptive, Nyquist criterion, and root locus.

Time domain (state-space) DPS control theory is based on semi-groups theory from functional analysis. Balas (1978) developed spillover bounds for a ROM-based controller/estimator for the generalized wave equation with damping, which can be used to guarantee DPS closed-loop stability. Sakawa (1983) obtained even sharper estimates on the influence of the spillover on the stability of the DPS system, but a functional observer was used. In Balas (1983), the controller was designed for a finite approximation of a class of DPS models using the Galerkin method. Pohjolainen (1982) derived necessary and sufficient conditions for the existence of a robust PI controller for a class of open-loop stable DPS. Mashkovskii (1983) proposed a method for approximation of a DPS with discrete spectrum by a ROM for synthesis of a modal control. Schumacher (1983) presented a design procedure for constructing stabilizing dynamic compensators for a class of DPS. Curtain (1985) developed estimates on spillover effects on all modes for pole placement methods. Jain (1987) proposed a new method for designing low-order compensators based on extended fractional representation and Youla parametrization. A generalization of LQG theory was given by Bernstein (1986). Gibson (1981), for a ROM based LQG, showed that as the order of the ROM is increased the control approaches the optimal control for the DPS. The interested reader can find several texts which treat in detail time-domain DPS control

theory, e.g. the mathematical framework which generalizes finite-dimensional control theory to DPS [Curtain 1978], exposition of some main areas in DPS control [Banks 1983], and a more applied presentation by Leipholtz (1986). The drawback of all the methods cited above is the assumption that the DPS model is known precisely, and hence the degree of robustness for these methods is very small.

Frequency domain DPS theory is based on complex algebra and transfer function algebra [Vidyasagar 1975, Desoer 1978, and Callier 1986]. The celebrated Nyquist criterion [Nyquist 1932] was generalized to MIMO systems [Desoer 1965, and Desoer 1968], extended to nonrational transfer functions [Callier 1972, Desoer 1975, MacFarlane 1977, MacFarlane 1988, Desoer 1980, and Chait 1988b], and simplified [Vidyasagar 1988]. Khatri (1970) developed a Popov-like criterion for DPS. Vidyasagar (1972) defined necessary and sufficient conditions for stability of a large class of DPS transfer functions. Again, it is assumed that the DPS model is known precisely in all the above cited publications.

It is well known that transfer functions of DPS can have nonminimum phase zeros [Wie 1981, Cannon 1984a, and Chait 1988c]. Arbitrary model truncation may not include these zeros and could give a false sense of stability for the full-order system. Hence, robustness of a ROM-based control method becomes essential.

In contrast to a ROM-based design, the collocated rate feedback method can increase system stability margin (i.e. damping) without having the spillover problem. This was shown using Lyapunov theory [Russel 1969, and Balas 1979], and the positive real lemma [Benhabib 1983]. The collocated rate feedback theory cannot guarantee stability of the closed-loop system in the presence of significant dynamics in the actuators and sensors. A "low authority" non-collocated rate

feedback has been suggested to moderately modify system behavior and reduce spillover effects [Auburn 1980]. Optimal passive control can be used to add damping to a DPS without sustaining spillover, but with limited effectiveness [Joshi 1980].

Several survey papers on theory and applications of DPS control are available. Ray (1978) surveyed applications of DPS theory to process control problems in industrial plants. Balas (1982) presented the mathematical framework and related topics in DPS control trends. An assessment of various contributions to control theory with applications to large space structures was given by Johnson (1983) and Nurre (1984). Applications to control of bridges and civil structures can be found in the text by Leipholz (1979).

Various techniques are available for minimizing spillover effects, assuming that the truncated model is also finite-dimensional. Orthogonal filters, rather than a mode shape based estimator, were used to better accommodate model errors (e.g. spillover) and certain disturbances [Skleton 1978]. Sesak (1979) used a quadratic performance criterion to minimize spillover of a finite set of modes. Spillover reduction by employing various state transformations and constraints were developed for an LQG controller [Calico 1979, and Longman 1979]. Another method obtained similar objective using optimal sensor placement [Barker 1986]. Chait (1988d) presented an augmented deterministic observer which includes spillover reducing filters.

The control problem of flexible robotic arms is somewhat more difficult. In addition to the infinite-dimensionality, the system is rotating, and thus is not self-adjoint under the usual inner-product. This excludes a series solution with orthogonal eigenmodes, which most DPS control theories rely on. This problem can be described in the context of unconstrained vs. constrained modeling approach [Hughes

1980, Hablani 1982, and Ulsoy 1984]. Because current theories for flexible robot control utilize the constrained approach [Cannon 1984a, Kanoh 1985, Rakhsha 1985, and Hastings 1987], ROM-based controllers suffer from the additional problem of mode coupling, resulting in spillover-like effects. A recent formulation presented a self-adjoint form which can be utilized in conjunction with ROM-based control methods to alleviate the mode coupling problem [Chait 1988e].

A recent direction in DPS theory is simultaneous robust stabilization of both the ROM and the DPS, based on frequency domain formulation. A general notion of robustness in a control system can be found in Doyle (1981) for lumped systems and in the text by Vidyasagar (1985) for a more general class of systems. Chen (1982) and Nett (1983) obtained sufficient and necessary conditions for robust stability, but good estimates for the degree of robustness were not given. The theory of  $H^\infty$  optimal sensitivity minimization has been generalized to include certain DPS, in particular delay systems [Foiás 1988]. The method developed in this dissertation is similar in spirit to the plant perturbation  $L_\infty$  bound-based methods in Glover (1986), Curtain (1986a,b), and Bontsema (1986), used to obtain the robustness degree. While the  $L_\infty$  methods cited above can be applied to MIMO systems, they do not provide a procedure for computation of the bounds and their approach for stability verification is different.

Experimental applications are found in large space structures and similar systems [Schaechter 1982, Bauldry 1983, Burke 1983, Radcliffe 1983, Sundararajan 1984, Auburn 1984, Hallauer 1985, Schafer 1985, and Ozguner 1987], in robotic arms [Cannon 1984a, and Kanoh 1985], in heating processes [Luasterer 1979, and Komine 1987], and in a boring bar machine [Klein 1975a,b]. Reading through the applications cited above, one can observe a striking similarity: *all* were distributed

parameter control systems but none employed a control similar to DPS control theories available in the literature. This might be understandable in large space structure applications, where no analytical model is available and the only information available is a ROM obtained from a finite-element method or from an identification procedure. In such systems, the only hope for spillover minimization is by utilizing some of the techniques discussed above. Nevertheless, models for the other systems cited above are available in the form of partial differential equations. Some possible reasons for not employing DPS control theory are that the theory is too abstract and thus not understood by the engineering community, or that it does not provide a reasonable degree of robustness, or that it requires actuators and sensors which cannot be implemented.

## 1.2. Objectives

The objectives of this dissertation were:

- i) develop a DPS control theory for a ROM-based control of a DPS which can be employed without a prerequisite understanding of sophisticated mathematics.
- ii) provide a "simple to define and compute" robustness measures with respect to model truncation errors and parameter variations.
- iii) allow classical frequency domain controller designs for rational transfer functions.

### 1.3. Organization of the Dissertation

An extended Nyquist stability criterion for DPS is developed in §2 in order to show stability of a DPS in the abstract. In §3, frequency domain bounds are developed for the truncation error of several classes of DPS. The extended Nyquist stability criterion is then modified to allow for truncated models and error bounds, and the concept of a "tube of uncertainty" is presented in §4. Classical frequency domain control designs for disturbance rejection and closed-loop magnitude shaping is discussed in §5. The results in §3-§5 are accompanied by several numerical examples. Following the conclusions are recommendations for future work. Some mathematical facts and theorems used in the dissertation are summarized in Appendix A. Relevant parts from the theory of the Laplace Transform pair are given in Appendix B.

## §2. EXTENDED NYQUIST STABILITY CRITERION FOR DISTRIBUTED PARAMETER SYSTEMS

In this chapter we develop an extended Nyquist stability criterion for nonrational transfer functions in the spirit of the classical Nyquist criterion [Nyquist 1932]. Recall that a necessary and sufficient condition for asymptotic stability of a rational transfer function is that all its poles lie in the open left half complex plane. This condition is easily verified using a partial fraction expansion of the transfer function which has a finite number of terms each asymptotically stable. However, this condition is only sufficient for stability of a nonrational transfer function. In fact, there exist transfer functions, nonrational and entire, that are not stable [Desoer 1965].

Several extensions to the classical Nyquist stability criterion are available [Desoer 1965, Callier 1972, Desoer 1980, Chait 1988b], for a system such as shown in Figure 2.1 with  $P(s)$  nonrational. These extensions differ in the assumptions made on  $C(s)$  and  $P(s)$  and on its impulse response  $p(t)$ . In [Desoer 1965], for  $C(s)=1$ ,  $p(t)$  is assumed to be bounded on  $[0, \infty)$ , absolutely integrable ( $L^1$ ) on  $[0, \infty)$ , and approaches zero as  $t \rightarrow \infty$ . In [Callier 1972], for  $C(s)=1$ , it is assumed that  $P(s)=P_a(s)+P_u(s)$ , where  $p_a(t)$  is  $L^1[0, \infty)$ , and where  $P_u(s)$  is rational and contains the poles of  $P(s)$  in  $\text{Re}(s) \geq 0$ . In [Chait 1988b], for proper  $C(s)$ , the assumptions are given in terms of  $P(s)$  only, in contrast to the above mentioned extensions. A generalization of the Nyquist criterion for matrix transfer functions [Desoer 1980] requires

similar assumptions as in [Desoer 1965] and a coprime factorization of  $P(s)$ .

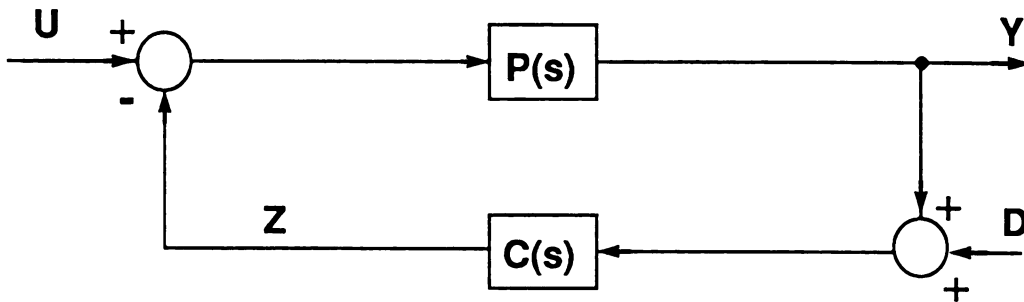


Figure 2.1: The feedback control system including measurement noise

All Nyquist stability criteria, classical and extended, require, in addition to the particular assumptions, that the encirclement condition is met by the Nyquist plot. In some cases, however, obtaining a complete Nyquist plot for a complicated transfer function in a transcendental form is difficult. This problem is solved in §4.

#### 2.1. Extended Nyquist Stability Criterion for SISO [Chait 1988b]

Consider the control system (typically used in control theory) shown in Figure 2.1. The system is described by the four transfer functions:  $Y(s)/U(s) \Delta H(s) = P(s)/[1+Q(s)]$ ,  $Y(s)/D(s) = -Q(s)/[1+Q(s)]$ ,  $Z(s)/U(s) = -Y(s)/D(s)$ , and  $Z(s)/D(s) = C(s)/[1+Q(s)]$ , where  $P(s)$  is possibly non-rational,  $Q(s) = P(s)C(s)$ , and where  $C(s)$  is a proper rational transfer function. It is often the case that  $P(s)$ , arising in a distributed parameter control system, satisfies, for some non-negative real constant  $\sigma_0$ , the following properties:

- (A1)  $P(s)$  is meromorphic in the finite right half-plane  $\text{Re}(s) \geq -\sigma_0$ ;
- (A2)  $P(s)$  and its first two derivatives are absolutely integrable

(L<sup>1</sup>) on the vertical line  $\text{Re}(s) = -\sigma_0$  outside some bounded sub-interval of the line;

(A3)  $P(s)$  and its first two derivatives vanish as  $|s| \rightarrow \infty$  on the closed right half-plane  $\text{Re}(s) \geq -\sigma_0$ .

(A4) There are no zero/pole cancelations in  $P(s)C(s)$  in the closed right half-plane  $\text{Re}(s) \geq -\sigma_0$ .

The results in this section are given for  $H(s)$  only. Results for the other three transfer functions follow from Theorem 2.2 and are given afterwards.

*Remark 2.1.*  $P(s)$  can include unstable elements. Delays are allowed as long as the above properties hold.

*Remark 2.2.*  $H(s)$  is meromorphic in  $\text{Re}(s) \geq -\sigma_0$  since the sum, product, and quotient of meromorphic functions are again meromorphic.

*Remark 2.3.*  $H(s)$  vanishes as  $|s| \rightarrow \infty$  on  $\text{Re}(s) \geq -\sigma_0$  because its denominator  $1+Q(s)$  is essentially 1 for large  $|s|$ . In fact,  $H(s)$  is dominated in magnitude by  $kP(s)$  on  $\text{Re}(s) \geq -\sigma_0$  for large  $|s|$  and some constant  $k$ . Likewise,  $H'(s)$  and  $H''(s)$  are dominated by certain derivatives of  $P(s)$  and thus vanish as  $|s| \rightarrow \infty$  on  $\text{Re}(s) \geq -\sigma_0$ .

*Remark 2.4.* Because  $H(s)$  is meromorphic and strictly proper on  $\text{Re}(s) \geq -\sigma_0$ , then  $H(s)$  can have at most a finite number of poles in  $\text{Re}(s) \geq -\sigma_0$ . As a result, the contour of the Nyquist graphical test can be finite.

For a stability theorem to make any sense at all, then existence, uniqueness, and causality of the closed-loop impulse response  $h(t)$  defined by the inversion formula

$$h(t) \triangleq \int_{-\sigma_0 - j\infty}^{-\sigma_0 + j\infty} H(s) e^{st} ds / 2\pi j = \int_{-\infty}^{\infty} H(-\sigma_0 + j\omega) e^{(-\sigma_0 + j\omega)t} d\omega / 2\pi, \quad (2.1)$$

must be demonstrated. We begin with a lemma showing that properties (A1)-(A4) plus a Nyquist-like criterion imply that  $H(s)$  is analytic on  $\text{Re}(s) \geq -\sigma_0$ . We then proceed to show existence, uniqueness, causality, and stability.

**Lemma 2.1.** Suppose that  $P(s)$  of a linear time-invariant system, shown in Figure 2.1, satisfies properties (A1)-(A4). If the Nyquist plot of  $Q(s)$  encircles the point  $(-1,0)$   $p_0$  times counterclockwise, where  $p_0$  denotes the number of poles of  $Q(s)$  in  $\text{Re}(s) > -\sigma_0$ , then  $H(s)$  is analytic on  $\text{Re}(s) \geq -\sigma_0$  (for a Nyquist plot definition see, for example, MacFarlane 1977).

**Proof.** By the Argument Principle [App. A],  $1+Q(s)$  has no zeros on  $\text{Re}(s) \geq -\sigma_0$ , and since  $H(s)$  is meromorphic on  $\text{Re}(s) \geq -\sigma_0$ , it follows that  $H(s)$  is analytic on  $\text{Re}(s) \geq -\sigma_0$ .

A system with a rational  $P(s)$  satisfying the hypotheses of Lemma 2.1 is stable since  $H(s)$  has no poles in  $\text{Re}(s) \geq -\sigma_0$ . However, as indicated earlier, this is only a necessary condition for a nonrational  $P(s)$  to be stable. The stability criterion extension for nonrational  $P(s)$  is given in the following theorem.

**Theorem 2.2.** If the hypotheses on  $P(s)$  given in Lemma 2.1 are satisfied, then the impulse response  $h(t)$  exists, is unique, causal, and asymptotically stable when  $\sigma_0=0$  and exponentially stable when  $\sigma_0>0$ .

**Proof.** *Existence:* Because  $H(s)$  is continuous and is dominated by  $P(s)$  on  $\text{Re}(s) \geq -\sigma_0$ , and since  $P(s)$  is, by A2, eventually  $L^1$  on  $\text{Re}(s) = -\sigma_0$ , then

$$\int_{-\infty}^{\infty} |H(-\sigma_0 + j\omega)| d\omega \leq \int_{-\Omega}^{\Omega} |H(-\sigma_0 + j\omega)| d\omega + k \int_{-\infty}^{-\Omega} |P(-\sigma_0 + j\omega)| d\omega + k \int_{\Omega}^{\infty} |P(-\sigma_0 + j\omega)| d\omega < \infty, \quad (2.2)$$

for some large positive  $\Omega$  and some positive constant  $k$ . Hence  $H(s)$  is  $L^1$  over the entire vertical line  $\text{Re}(s) = -\sigma_0$ . Thus the integral (2.1) converges absolutely.

*Causality:* Because  $H(s)$  is analytic on  $\text{Re}(s) \geq -\sigma_0$ , by the Cauchy Theorem [App. A] the integral (2.1) can be separated into three contour integrals as follows

$$h(t) = \int_{\Gamma} H(s) e^{st} ds / 2\pi j + e^{-\sigma_0 t} \int_{\Omega}^{\infty} H(-\sigma_0 + j\omega) e^{j\omega t} d\omega / 2\pi + e^{-\sigma_0 t} \int_{-\infty}^{-\Omega} H(-\sigma_0 + j\omega) e^{j\omega t} d\omega / 2\pi, \quad (2.3)$$

where  $\Omega$  is a large positive number and  $\Gamma$  denotes the semicircle  $s = -\sigma_0 + \Omega e^{j\theta}$ ,  $-\pi/2 \leq \theta \leq \pi/2$ . Because  $H(s)$  vanishes as  $|s| \rightarrow \infty$  on  $\text{Re}(s) \geq -\sigma_0$ , the Jordan Lemma [App. A] guarantees that the integral along  $\Gamma$  approaches zero as  $\Omega \rightarrow \infty$  for  $t < 0$ . Because  $H(-\sigma_0 + j\omega)$  is  $L^1$ , the last two integrals can be made arbitrary small for sufficiently large  $\Omega$ . Therefore,  $h(t) = 0$  for  $t < 0$ .

An easier but non-traditional proof of causality can be obtained by employing a rectangular contour rather than the above semi-circle employed in the Jordan Lemma. This proof is given in Appendix B.

*Remark 2.5.* Because  $H(s)$  is  $L^1$ ,  $h(t)$  is continuous by the Lebesgue Bounded Convergence Theorem [App. A].

*Stability:* Because of Remark 3, Lemma 2.1, and property A2, integrating the inversion formula (2.1) twice by parts yields, for  $t > 0$ ,

$$\begin{aligned}
 e^{\sigma_0 t} h(t) &= \int_{-\infty}^{\infty} H(-\sigma_0 + j\omega) e^{j\omega t} d\omega / 2\pi \\
 &= H(-\sigma_0 + j\omega) / (2\pi) \frac{e^{j\omega t}}{jt} \Big|_{-\infty}^{\infty} - \frac{1}{t} \int_{-\infty}^{\infty} H'(-\sigma_0 + j\omega) e^{j\omega t} d\omega / 2\pi \\
 &= -H'(-\sigma_0 + j\omega) / (2\pi) \frac{e^{jt}}{jt^2} \Big|_{-\infty}^{\infty} + \frac{1}{t} \int_{-\infty}^{\infty} H''(-\sigma_0 + j\omega) e^{j\omega t} d\omega / 2\pi \\
 &= \frac{1}{t^2} \int_{-\infty}^{\infty} H''(-\sigma_0 + j\omega) e^{j\omega t} d\omega / 2\pi . \tag{2.4}
 \end{aligned}$$

The following notation is used  $H'(\cdot) = dH(\cdot)/d\omega$ . The product  $e^{\sigma_0 t} h(t)$  is in  $L^1[0, \infty)$  since the function on the right hand side of Eqn. (2.4) is of order  $1/t^2$  at  $\infty$ . Thus  $h(t)$  is asymptotically stable when  $\sigma_0 \geq 0$  and exponentially stable when  $\sigma_0 > 0$ . By asymptotic stability we mean bounded-input bounded-output stability plus  $h(t) \rightarrow 0$  as  $t \rightarrow \infty$  (for stability definitions see App. A).

*Uniqueness:* Because both  $H(s)$  and  $h(t)$  are absolutely integrable and since  $H(s)$  is differentiable, then by [Doetsch 1970],  $h(t)$  and  $H(s)$  are a Laplace transform pair.

A second proof of the theorem can be obtained by appeal to the results in [Desoer 1975, Desoer 1980]. Splitting off the unstable singular part from  $Q(s)$  to obtain a residual part analytic on  $\text{Re}(s) \geq -\sigma_0$ , and by employing at times conditionally convergent integral, it can be shown that the inverse Laplace transform of  $Q(s)$  belongs to the class of systems considered there. Thus our hypotheses can be employed to decide whether or not a non-rational transfer function is covered

there. Our analysis also provides an independent proof for closed-loop impulse response stability.

The results for the transfer function  $Q(s)/[1+Q(s)]$  follow by similar arguments used in the proof of Theorem 2.2 and are given in the following corollary.

**Corollary 2.3.** If the hypothesis given in Theorem 2.2 is satisfied, then the conclusions of Theorem 2.2 also hold for the impulse response of  $Q(s)/[1+Q(s)]$ .

To consider the fourth transfer function  $F(s)\Delta C(s)/[1+Q(s)]$ , we must consider stability in the generalized sense [MacCluer 1988b].

**Corollary 2.4.** If the hypothesis given in Theorem 2.2 is satisfied and  $C(s)$  is analytic on  $\text{Re}(s) \geq -\sigma_0$ , then  $f(t)$  is stable in the generalized sense [MacCluer 1988b]. Moreover, if  $C(s)$  is strictly proper,  $f(t)$  is asymptotically stable when  $\sigma_0=0$  and exponentially stable when  $\sigma_0>0$ .

**Proof.** In the time-domain, the impulse response  $f(t)$  is given by

$$f(t) = c(t) - c(t) * c(t) * h(t), \quad (2.5)$$

where '\*' denotes generalized convolution [MacCluer 1988]. Because  $C(s)$  is proper,  $f(t)$  is the difference of bounded-input bounded-output stable impulse responses. Moreover, if  $C(s)$  is strictly proper, then  $c(t)$  is exponentially stable. Therefore, because of Equation (2.5),  $f(t)$  and  $h(t)$  share stability type. Note that  $C(s)$  is not required to be stable in Theorem 2.2 and in Corollary 2.3.

## 2.2. Extended Nyquist Stability Criterion for MIMO [Smith 1984]

A generalization of the above extended criterion to the MIMO case where  $P(s)$  and  $C(s)$  are matrix transfer functions can be obtained using the return-difference matrix

$$F(s) = I + P(s)C(s) = I + Q(s). \quad (2.6)$$

The conditions for analyticity of  $\text{Det}[F(s)]$ , which replaces the polynomial  $1+Q(s)$  in Lemma 2.1, are presented in the following theorem.

**Theorem 2.3.** Suppose that  $Q(s)$  has  $p_0$  poles in  $\text{Re}(s) \geq \sigma_0$ . Then  $\text{Det}[F(s)]$  is analytic on  $\text{Re}(s) > -\sigma_0$  if and only if the number of counterclockwise encirclements of the origin by the Nyquist diagram of  $\text{Det}[F(s)]$  is equal to  $p_0$ .

There may be cancelations between the numerator and denominator of  $[F(s)]^{-1} = \text{Adj}[F(s)]/\text{Det}[F(s)]$ . When each of the entries in the matrices  $P(s)$  and  $C(s)$  satisfies the hypothesis in Thm. 2.2 and Corollaries 2.3-2.4, then their corresponding conclusions should hold for the matrix transfer functions  $H(s) = P(s)[F(s)]^{-1}$ ,  $Q(s)[F(s)]^{-1}$ , and  $C(s)[F(s)]^{-1}$ . The details are left for future work.

### §3. FREQUENCY DOMAIN TRUNCATION BOUNDS

In this chapter truncation error bounds are developed for systems whose dynamics can be represented by a series solution, where each term in the series arises from a first or second order ordinary differential equation. Truncation of higher order terms from the series solution yields errors which must be considered in any control design that is essential in any realistic control implementation. It is assumed here that the truncated model includes all the unstable terms (modes) of the open-loop system. This assumption is necessary if the control objective is to stabilize unstable modes or improve performance of the system.

#### 3.1. Bounds for First Order Terms [Chait 1988a]

Consider the following transfer function

$$G(s) = \sum_{k=1}^m \frac{\delta_k}{s + \tau_k} , \quad (3.1)$$

where  $m$  is finite or infinite,  $\delta_k$  are bounded real numbers, and  $\tau_k = c_k k^\rho$  where both  $\rho$  and  $c_k$  are positive reals,  $k=1,2,\dots$ . The transfer function (3.1) is nonrational if  $m=\infty$  and rational if  $m<\infty$ . Without loss of generality we consider a truncated, rational, transfer function obtained by retaining the first  $n$  terms in Equation (3.1) while the remaining terms, infinite in number, are neglected:

$$G_n(s) = \sum_{k=1}^n \frac{\delta_k}{s + \tau_k}, \quad n < m. \quad (3.2)$$

This method of truncation is not unique, in fact, one can retain any finite number of modes in  $G_n(s)$ . The following results hold for  $G_n(s)$  obtained from any finite truncation method.

For frequency domain stability analysis, the transfer function is converted to a frequency response function (FRF) by letting  $s=j\omega$ , where  $\omega$  denotes the frequency. Define a truncation error  $E(j\omega)$  as

$$E(j\omega) \triangleq G(j\omega) - G_n(j\omega) = \sum_{k=n+1}^m \frac{\delta_k}{j\omega + \tau_k}, \quad n < m. \quad (3.3)$$

**A Uniform Bound.** Consider the modulus of the  $k^{\text{th}}$  term of the FRF (3.3)

$$|S_k(j\omega)| = \frac{|\delta_k|}{\sqrt{\omega^2 + \tau_k^2}}. \quad (3.4)$$

The modulus  $|S_k(j\omega)|$  has a supremum over  $\omega \in [0, \infty)$  equal to  $|\delta_k|/\tau_k$ , the DC gain of the FRF. The uniform bound for the truncation error modulus is thus defined as

$$|E(j\omega)| \leq \delta \sum_{k=n+1}^m \frac{1}{\tau_k} \triangleq R_1, \quad \omega \in (-\infty, \infty), \quad (3.5)$$

where  $\delta \triangleq \sup\{|\delta_k| \neq 0, k=n+1, \dots, m\}$ . Note that the series with  $m=\infty$  will converge only if  $\rho > 1$  and the sequence  $(\tau_k)$  is bounded below. The uniform bound provides a constant nonzero bound for all  $\omega \geq 0$ .

**A Frequency Dependent Bound.** A bound that approaches zero as the frequency approaches infinity can be derived for the FRF (3.3). The modulus of the  $k^{\text{th}}$  term can be bounded as follows

$$|S_k(j\omega)| = \frac{|\delta_k|}{\sqrt{\omega^2 + r_k^2}} \leq \frac{1}{\omega^\alpha} \sup_{\omega} \left| \frac{\omega^\alpha |\delta_k|}{\sqrt{\omega^2 + r_k^2}} \right|, \quad \omega \neq 0, \quad (3.6)$$

where  $0 < \alpha < 1$ , and where  $\sup|\cdot|$  denotes the supremum over  $\omega \in [0, \infty)$  for a fixed  $k$ . It can be shown that

$$\sup \left| \frac{\omega^\alpha |\delta_k|}{\sqrt{\omega^2 + r_k^2}} \right| = |\delta_k| (\alpha)^{\alpha/2} (1-\alpha)^{(1-\alpha)/2} \frac{1}{r_k^\beta}, \quad (3.7)$$

where  $\beta = 1 - \alpha$ . The frequency dependent bound for the truncation error modulus is thus defined as

$$|E(j\omega)| \leq \frac{\delta}{\omega^\alpha} (\alpha)^{\alpha/2} (1-\alpha)^{-\alpha} \sum_{k=n+1}^m \frac{1}{r_k^\beta} \triangleq R_2(\omega), \quad \omega \in (-\infty, \infty), \quad (3.8)$$

where  $\delta \triangleq \sup(|\delta_k|) \neq 0, k=n+1, \dots$ . The sum exists when  $\beta - \alpha > 1$ . This bound increases for decreasing frequencies below one and approaches zero as  $\omega \rightarrow \infty$ .

### 3.2. Bounds for Second Order Terms [Chait 1988a]

Consider the following transfer function

$$G(s) = \sum_{k=1}^m \frac{\delta_k}{s^2 + 2\zeta_k \omega_k s + \omega_k^2}, \quad (3.9)$$

where  $m$  is finite or infinite, both  $\rho$  and  $c_k$  are positive real,  $\delta_k$  are bounded real numbers,  $\omega_k = c_k k^\rho$  are the natural frequencies, and  $\zeta_k$  are the modal damping factors for underdamped transfer functions with overshoot:  $0 < \epsilon_1 \leq \zeta_k \leq \epsilon_2 < 0.707$ ,  $k=1, 2, \dots$ . Whenever  $\zeta_k > 0.707$  one can show that a resonant peak in the FRF magnitude does not exist. Thus there is no magnification and both bounds are computed as shown in Section 3.1 for first order terms. A typical truncated rational transfer function was obtained in Section 3.1. The truncation error  $E(j\omega)$  is here defined as

$$E(j\omega) \triangleq G(j\omega) - G_n(j\omega) = \sum_{k=n+1}^m \frac{\delta_k}{(\omega_k^2 - \omega^2) + j2\zeta_k \omega_k \omega}, \quad n < m. \quad (3.10)$$

**A Uniform Bound.** Consider the modulus of the  $k^{\text{th}}$  term of the FRF  
(3.10)

$$|S_k(j\omega)| = \frac{\delta_k}{\sqrt{(\omega_k^2 - \omega^2)^2 + (2\zeta_k \omega_k \omega)^2}} = \frac{\delta_k}{\omega_k^2 \sqrt{f_k(\omega)}}, \quad (3.11)$$

where

$$f_k(\omega) \triangleq [1 - \omega^2/\omega_k^2]^2 + [2\zeta_k \omega/\omega_k]^2. \quad (3.12)$$

The modulus  $|S_k(j\omega)|$  has a supremum over  $\omega \in [0, \infty)$  exactly when  $f_k(\omega)$  has a infimum there. A simple algebraic rearrangement yields [Ogata 1970]

$$f_k(\omega) = \left[ \frac{\omega^2 - \omega_k^2(1-2\zeta_k^2)}{\omega_k^2} \right]^2 + 4\zeta_k^2(1-\zeta_k^2), \quad (3.13)$$

and by inspection, the infimum of  $f_k(\omega)$  occurs when  $\omega = \omega_k \sqrt{1-2\zeta_k^2}$ . Thus the uniform bound for the modulus of a single FRF  $S_k(j\omega)$  is

$$|S_k(j\omega)| \leq \frac{\delta_k}{2\omega_k^2 \zeta_k \sqrt{1-\zeta_k^2}}, \quad \omega \in [0, \infty). \quad (3.14)$$

The uniform bound for the truncation error modulus is thus defined as

$$|E(j\omega)| \leq \frac{\delta}{\Gamma_1} \sum_{k=n+1}^m \frac{1}{\omega_k^2} \triangleq R_1, \quad \omega \in (-\infty, \infty), \quad (3.15)$$

where  $\delta \triangleq \sup(|\delta_k|) \neq 0$ , and  $\Gamma_1 \triangleq \inf(2\zeta_k \sqrt{1-2\zeta_k^2}) \neq 0$   $k=n+1, \dots$ . The series converges for  $m \rightarrow \infty$  only if  $\rho > 0.5$  and the sequence  $\{c_k\}$  is bounded above from zero.

It is a common practice in control analysis to assume that the modal damping factor  $\zeta_k$  is a constant for all terms (modes). However, the uniform bound (3.15) allows for a wide variation in the damping ratio for different terms which agrees with experimental results [Breakwell 1983]. To compute this bound it is sufficient to know the constants  $\epsilon_1$  and  $\epsilon_2$ , giving  $\Gamma_1 = \min(\epsilon_i \sqrt{1-2\epsilon_i^2})$ ,  $i=1,2$ . Therefore, this bound is robust to modal damping variations in different terms and allows flexibility in compensator design. The uniform bound provides a constant nonzero bound for all frequencies.

**A Frequency Dependent Bound.** A bound that approaches zero as the frequency approaches infinity can be derived for the FRF (3.10).

Consider the modulus of the  $k^{\text{th}}$  term rearranged to

$$|T_k(j\omega)| = \frac{\delta_k}{\omega \omega_k \sqrt{h_k(\omega)}} , \quad (3.16)$$

where

$$h_k(\omega) = \left[ \frac{\omega_k^2 - \omega^2}{\omega_k \omega} \right]^2 + 4\zeta_k^2 . \quad (3.17)$$

The modulus  $|T_k(j\omega)|$  can be bounded above using the inequality

$|T_k(j\omega)| \leq (1/\omega\omega_k) \inf(\sqrt{h_k(\omega)})$ ,  $\omega \in [0, \infty)$ . The infimum of  $h_k(\omega)$  occurs when  $\omega = \omega_k$  giving

$$|T_k(j\omega)| \leq \frac{\delta_k}{2 \omega \omega_k \zeta_k} , \quad \omega \in (0, \infty) . \quad (3.18)$$

The frequency dependent bound for the truncation error modulus is thus defined as

$$|E(j\omega)| \leq \frac{\delta}{\Gamma_2 \omega} \sum_{k=n+1}^m \frac{1}{\omega_k} \triangleq R_2(\omega) , \quad \omega \in (-\infty, \infty) , \quad (3.19)$$

where  $\Gamma_2 \triangleq \inf(2\zeta_k) = 2\epsilon_1 \neq 0$ , and  $\gamma \triangleq \sup(\alpha_k \beta_k) \neq 0$ ,  $k=1, 2, \dots$ .



### 3.3. Overall Bound [Chait 1988a]

The smaller of the bounds  $R_1$  and  $R_2(\omega)$  can be used over different frequency ranges to produce a smaller overall bound (Figure 3.1). Note that as more terms (modes) are included in the truncated model, both bounds decrease with limit zero as  $n \rightarrow \infty$ . Both bounds are robust to modal damping variations in different terms.

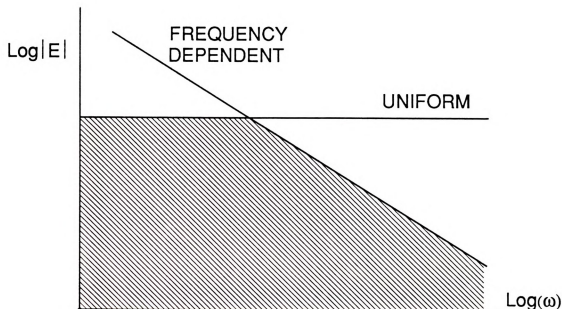


Figure 3.1: The truncation bounds

### 3.4. Bounds for Terms About Any Vertical Axis

When closed-loop exponential stability is desired, similar error bounds for first and second order terms must be developed about a vertical line to the left of the imaginary axis. The bounds derived below are similar to the bounds derived in Sections 3.1 and 3.2.



**First Order Terms.** Consider the following transfer function

$$G(s-\sigma_0) = \sum_{k=1}^m \frac{\delta_k}{s - \sigma_0 + \tau_k}, \quad (3.20)$$

where  $\sigma_0$  is a nonnegative real number,  $m$  is finite or infinite, and  $\delta_k$  and  $\tau_k$  are defined as in Section 3.1. This transfer function is equivalent to the transfer function (3.1) with a modified root  $\tilde{\tau}_k \triangleq \tau_k - \sigma_0$  (Figure 3.2).

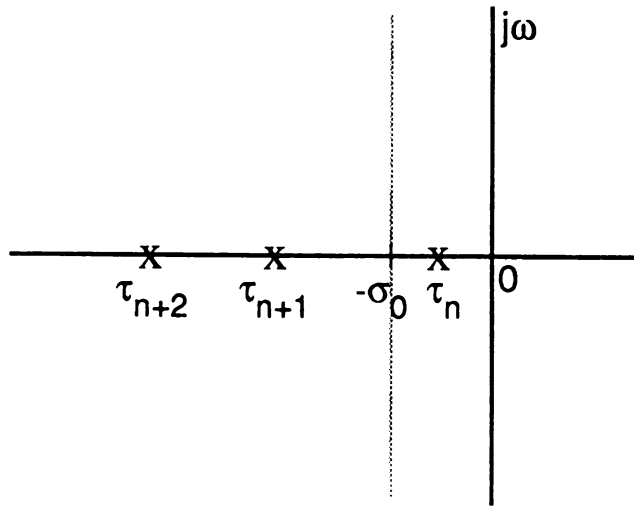


Figure 3.2: The modified first order root

Following the derivation in Section 3.1, the uniform bound for the truncation error modulus of the FRF (3.20) is thus defined as

$$|E(j\omega)| \leq \delta \sum_{k=n+1}^m \frac{1}{\tilde{\tau}_k} \triangleq R_1, \quad \omega \in (-\infty, \infty), \quad (3.21)$$



where  $\delta \Delta \sup(|\delta_k|)$ ,  $k=n+1, \dots$ . This bound has a meaning only if  $\tau_k > \sigma_0$  for all  $k \geq n+1$ . The frequency dependent bound is defined as

$$|E(j\omega)| \leq \frac{\delta}{\omega^\alpha} (\alpha)^{\alpha/2} (1-\alpha)^{(1-\alpha)/2} \sum_{k=n+1}^m \frac{1}{\tilde{\tau}_k^\beta} \Delta R_2(\omega), \quad \omega \in (-\infty, \infty), \quad (3.22)$$

where  $\delta \Delta \sup(|\delta_k|) \neq 0$ ,  $\rho - \beta > 1$ ,  $0 < \alpha < 1$ ,  $\beta = 1 - \alpha$ ,  $k = n+1, \dots$ .

**Second Order Terms.** Consider the following transfer function

$$G(s - \sigma_0) = \sum_{k=1}^m \frac{\delta_k}{(s - \sigma_0)^2 + 2\zeta_k \omega_k (s - \sigma_0) + \omega_k^2}, \quad (3.23)$$

where  $\sigma_0$  is a nonnegative real constant,  $m$  is finite or infinite, and  $\delta_k$ ,  $\omega_k$ , and  $\zeta_k$  are defined in Section 3.2. This second order system is similar to the system in Equation (3.9) with modified natural frequencies  $\omega_k = \tilde{\omega}_k$  and damping ratios  $\zeta_k = \tilde{\zeta}_k$  (Figure 3.3). We first derive intermediate bounds for  $\tilde{\omega}_k$  and  $\tilde{\zeta}_k$ . From Figure 3.3 it is clear that

$$\tilde{\omega}_k^2 \Delta \omega_k^2 (1 - \zeta_k) + (\zeta_k \omega_k - \sigma_0)^2 \geq (\omega_k - \sigma_0)^2, \quad \zeta_k < 1, \quad (3.24)$$

and hence,

$$1/\tilde{\omega}_k \leq 1/\omega_k - \sigma_0, \quad \omega_k > \sigma_0. \quad (3.25)$$

This bound should be used for terms whose real part is located to the left of the shifted imaginary axis, i.e.  $\zeta_k \omega_k > \sigma_0$ . When  $\sigma_0 > 0$ , the range



of the modified damping ratio  $\tilde{\zeta}_k$  is changed. Clearly,  $\tilde{\epsilon}_1 \leq \epsilon_1$  and  $\tilde{\epsilon}_2 \leq \epsilon_2$ . Using  $\text{Cos}[\phi] \Delta \zeta_k$ , Equation (3.25), and Figure 3.3 we obtain bounds for the modified range  $\tilde{\zeta}_k \in [\tilde{\epsilon}_1, \tilde{\epsilon}_2]_k$ . For each fixed  $k$  we have

$$\text{Cos}[\phi_k] \geq \inf\{(\zeta_k \omega_k - \sigma_0)/\tilde{\omega}_k\} = (\epsilon_1 \omega_k - \sigma_0)/\tilde{\omega}_k \triangleq \tilde{\epsilon}_{1k} , \quad (3.26a)$$

and

$$\text{Cos}[\phi_k] \leq \sup\{(\zeta_k \omega_k - \sigma_0)/\tilde{\omega}_k\} = (\epsilon_2 \omega_k - \sigma_0)/\tilde{\omega}_k \triangleq \tilde{\epsilon}_2 . \quad (3.26b)$$

Note that both  $\inf\{\tilde{\epsilon}_1\}$  and  $\inf\{\tilde{\epsilon}_2\}$  for  $k > n+1$  occur when  $k=n+1$ , and that the sector in the second quadrant defined by the pair  $(\tilde{\epsilon}_1, \tilde{\epsilon}_2)_k$  is being reoriented toward the imaginary axis. The modified range is thus defined by

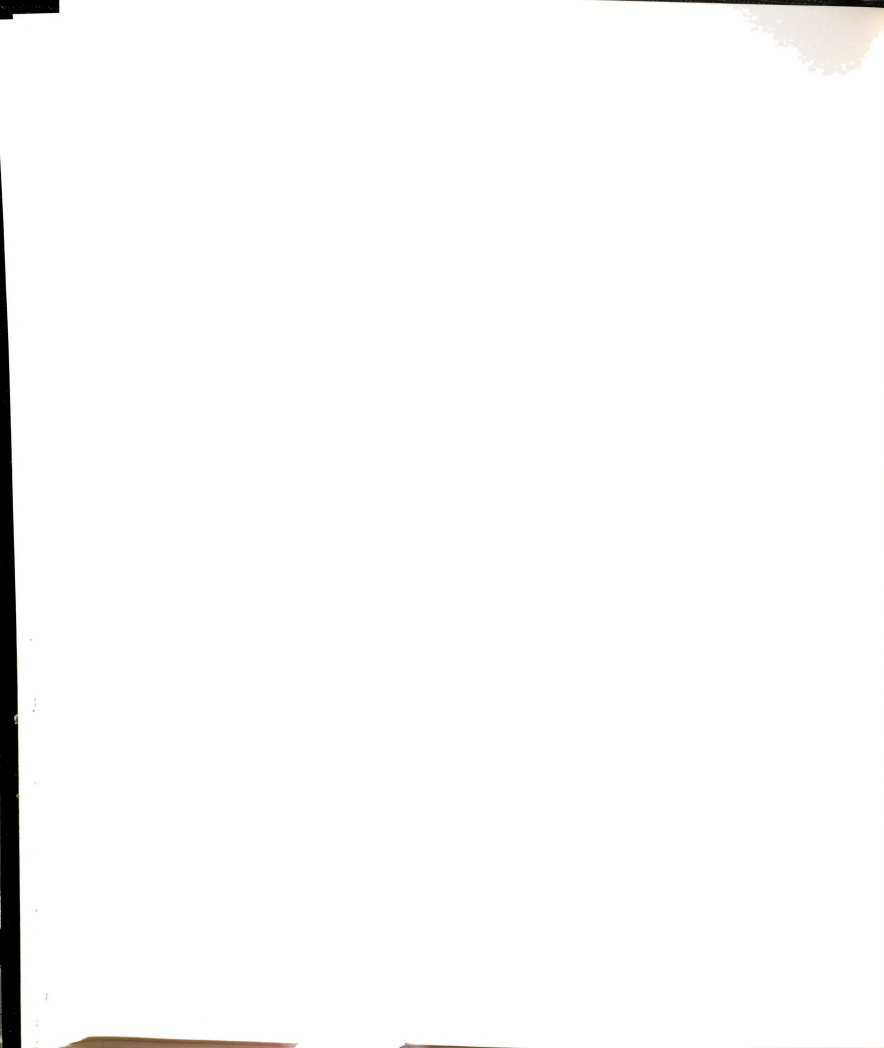
$$\tilde{\epsilon}_1 \triangleq (\epsilon_1 \omega_{n+1} - \sigma_0)/\omega_{n+1} \quad \text{and} \quad \tilde{\epsilon}_2 \triangleq (\epsilon_2 \omega_{n+1} - \sigma_0)/\omega_{n+1} . \quad (3.27)$$

Also note that  $(\tilde{\epsilon}_1, \tilde{\epsilon}_2)_k \rightarrow (\epsilon_1, \epsilon_2)$  as  $k \rightarrow \infty$ ,  $|\sigma_0| < \infty$ . Following the derivation in Section 3.2, we define a uniform bound for the truncation error modulus of a FRF (3.23)

$$|E(-\sigma_0 + j\omega)| \leq \frac{\delta}{\tilde{\Gamma}_1} \sum_{k=n+1}^m \frac{1}{\tilde{\omega}_k^2} \triangleq R_1 , \quad \omega \in (-\infty, \infty), \quad (3.28)$$

where  $\delta \triangleq \sup\{|\delta_k|\} \neq 0$ ,  $\tilde{\Gamma}_1 \triangleq \inf\{2\tilde{\epsilon}\sqrt{1-2\tilde{\epsilon}^2}\} \neq 0$ ,  $\tilde{\epsilon} \in [\tilde{\epsilon}_1, \tilde{\epsilon}_2]$ , and  $k=n+1, \dots$ .

The frequency dependent bound is defined as



$$|E(-\sigma_0 + j\omega)| \leq \frac{\delta}{\bar{\Gamma}_2 \omega} \sum_{k=n+1}^m \frac{1}{\tilde{\omega}_k} \triangleq R_2(\omega), \quad \omega \in (-\infty, \infty), \quad (3.29)$$

where  $\delta \triangleq \sup(|\delta_k|) \neq 0$ , and  $\bar{\Gamma}_2 \triangleq \inf(2\tilde{\zeta}_k) = 2\tilde{\epsilon}_1$ ,  $k=n+1, \dots$ .

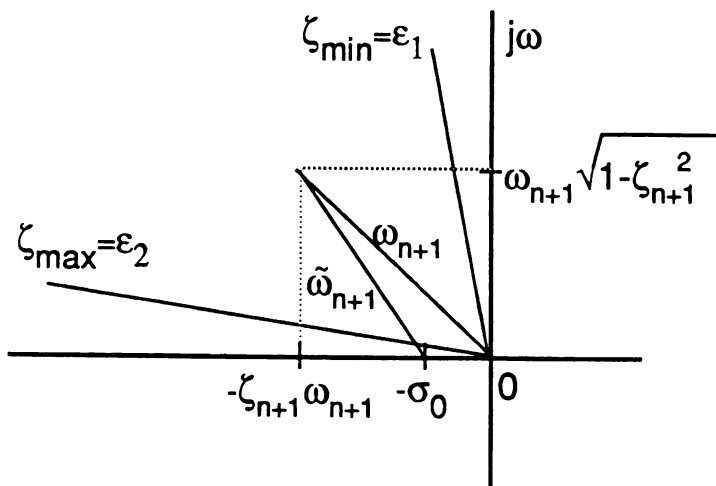


Figure 3.3: The modified second order root

### 3.5. Numerical Computation of the Bounds

The numerical computation of the bounds (3.5), (3.15), and (3.19) is often straight forward. Sums for series with  $m \rightarrow \infty$  and  $\sigma_0 = 0$  are tabulated for different integer powers  $\rho$  in many mathematical handbooks [Beyer 1982]. Let  $c_k = 1$  in this section. When  $\rho$  is positive real one can resort to the inequality employed in the Integral Test [Trench 1978]

$$\int_1^{m+1} x^{-\rho} dx \leq \sum_{k=1}^m k^{-\rho} \leq 1^{-\rho} \int_1^m x^{-\rho} dx, \quad (3.30)$$

for some integer  $1 < m$ . Additional work is required to compute the bounds (3.21), (3.28) and (3.29). To do so, consider the series

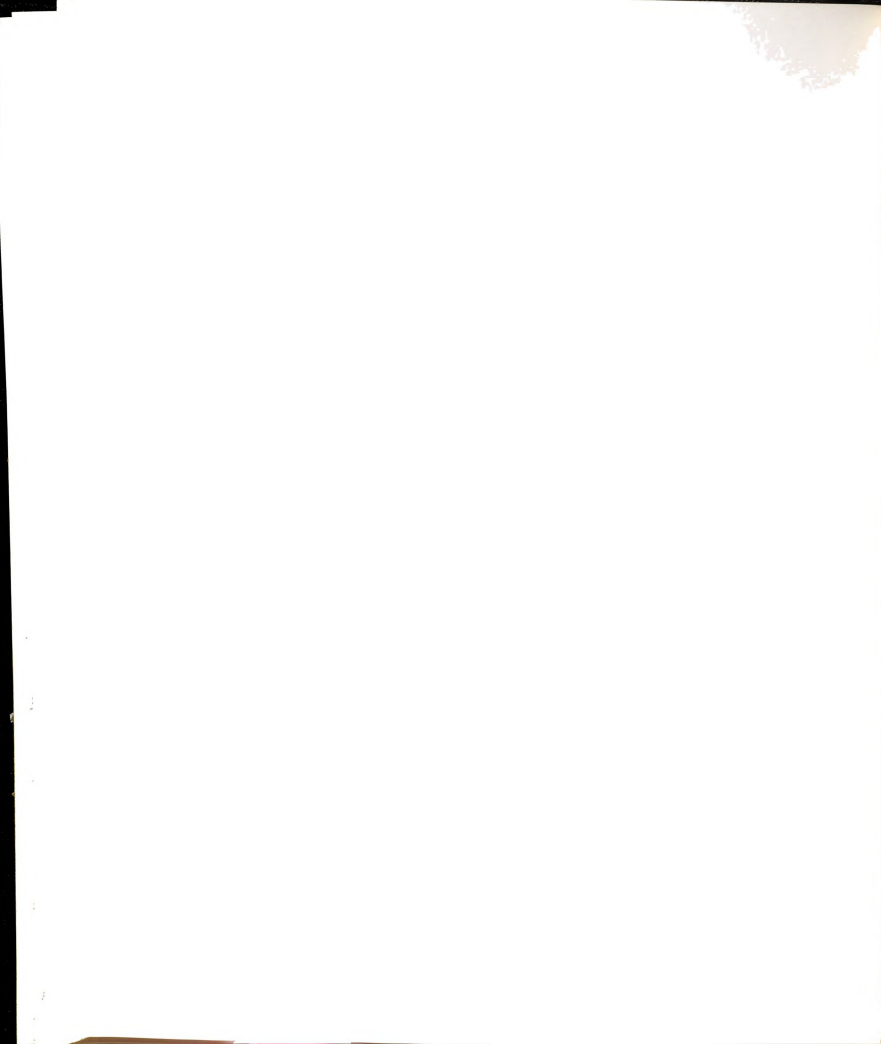
$$\sum_{k=1}^m \frac{1}{k^{\rho-\sigma_0}} = \sum_{k=1}^m \frac{k^{\rho}}{k^{\rho-\sigma_0}} \frac{1}{k^{\rho}} \leq \left| \frac{k^{\rho}}{k^{\rho-\sigma_0}} \right|_{\infty} \sum_{k=1}^m \frac{1}{k^{\rho}}, \quad (3.31)$$

where  $\rho > 1$ ,  $\sigma_0$  is a nonnegative constant,  $k^{\rho} > \sigma_0$ , and  $|\cdot|_{\infty}$  denotes the supremum over  $k$ . The inequality (3.31) implies that the series on the left is absolutely convergent by the Comparison Test [Trench 1978]. The sum for  $\sigma_0 > 0$  is bounded above by the sum for  $\sigma_0 = 0$  multiplied by the factor  $\left| k^{\rho} / (k^{\rho} - \sigma_0) \right|_{\infty}$ . This factor monotonically decreases toward a limit of one as  $k \rightarrow \infty$ . Thus, in a series truncated after  $n$  terms,  $|\cdot|_{\infty} \Delta(n+1)^{\rho} / [(n+1)^{\rho} - \sigma_0]$ .

### 3.6. Graphical Interpretation of the Error Bounds [Chait 1988a]

The nonrational FRF  $G(j\omega)$  is within the error bounds  $R_1$  and  $R_2$  of the truncated (rational) FRF  $G_n(j\omega)$ . At each frequency,  $G(j\omega)$  is within circles of radii  $R_1$  and  $R_2(\omega)$ , centered at the point  $G_n(j\omega)$  (Figure 3.4). Therefore,  $G(j\omega)$  always lies within the smaller of the two circles. That circle represents the uncertainty due to the order truncation.

The polar plot for  $G(j\omega)$  over a range of frequencies has a similar interpretation. The polar plot  $G_n(j\omega)$  is drawn together with error circles associated with each frequency in that range. The union of all the smaller error circles defines two plots: an interior boundary and an exterior boundary. The polar plot of  $G(j\omega)$  is then found within that **tube of uncertainty**, enclosed by the interior and exterior



boundaries (Figure 3.4). The tube of uncertainty represents a bound on model truncation error in the frequency domain. The tube of uncertainty corresponds, in an abstract sense, to spillover bounds [Balas 1978] and Gershgorin discs [Franke 1985] in the time domain.

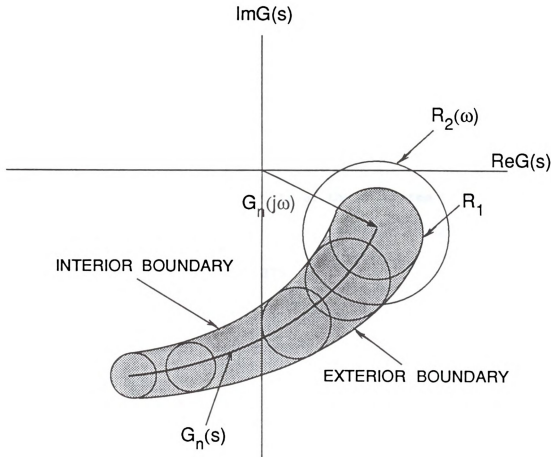


Figure 3.4: Bound circles and the tube of uncertainty

### 3.7. Numerical Example: Error Bounds Calculation [Chait 1988a]

Consider a transfer function of the form (3.11) with  $m=\infty$ ,  $\omega_k=(k\pi)^2$ ,  $\delta=2$ ,  $\epsilon_1=0.005$ , and  $\epsilon_2=0.5$ . This transfer function corresponds to the ratio between a position point sensor to a point actuator of the Bernoulli-Euler beam with unity parameters.



The uniform bound,  $R_1$ , and the frequency dependent bound,  $R_2(\omega)$ , can be calculated for  $\sigma_0=0$  using Equations (3.15) and (3.19) since  $\rho=2$ . For this system we have:  $\delta=2$ , and  $\Gamma_1=\Gamma_2=0.01$ . For a truncated series which consists of the first term ( $n=1$ ) alone:

$$R_1 = 200 \sum_{k=2}^{\infty} \frac{1}{(k\pi)^4} \approx 0.1692 \quad (3.32)$$

and

$$R_2(\omega) = \frac{200}{\omega} \sum_{k=2}^{\infty} \frac{1}{(k\pi)^2} \approx \frac{13.18}{\omega} \quad (3.33)$$

For a truncated series which consists of the first ten terms ( $n=10$ ):

$$R_1 = 200 \sum_{k=11}^{\infty} \frac{1}{(k\pi)^4} \approx 0.00000373 \quad (3.34)$$

and

$$R_2(\omega) = \frac{200}{\omega} \sum_{k=11}^{\infty} \frac{1}{(k\pi)^2} \approx \frac{0.0102}{\omega} \quad (3.35)$$

For the transfer function considered in this example and a shifted imaginary axis by  $\sigma_0=0.1$  we can compute similar bounds. For  $n=1$ , since  $\zeta_2\omega_2>0.1$  we can use Equations (3.26a) and (3.26b) to compute  $\tilde{\epsilon}_1=0.00246$  and  $\tilde{\epsilon}_2=0.497$ . Using the result of Section 3.5 we compute the modified bounds for  $n=1$ :  $R_1=0.344$  and  $R_2(\omega)=26.79/\omega$ . For  $n=10$  since  $\zeta_{11}\omega_{11}>0.1$  we compute  $\tilde{\epsilon}_1=0.0049$  and  $\tilde{\epsilon}_2=0.497$ , and the modified bounds are:  $R_1=0.00000381$  and  $R_2(\omega)=0.0104/\omega$ . Note that the effect of shifting the imaginary axis on the bounds becomes larger as the axis is shifted closer to the  $(n+1)^{\text{th}}$  root.

#### §4. FREQUENCY DOMAIN STABILITY ANALYSIS USING TRUNCATED MODELS

In this chapter a practical Nyquist stability criterion is developed for nonrational transfer functions based on truncated, rational models and truncation error bounds. The results below are based on Nyquist stability results from §2 and truncation error bounds and tube of uncertainty from §3.

##### 4.1. Generation of Nyquist Plots [Chait 1988a,c]

Consider a typical SISO control system shown in Figure 4.1 which includes a disturbance at the DPS input. This figure is different from Figure 2.1 which includes measurement noise since typically a controller is added in order to attenuate the undesirable effects of disturbances. The general stability theory developed in §2 also applies to this block diagram configuration. Let  $P(s)=G_c(s)G(s)$  and  $C(s)=G_f(s)$  satisfy the hypothesis given in Theorem 2.2. Let  $G_n(s)$  be a rational approximation (truncation) of  $G(s)$ , such that  $G(s)$  and  $G_n(s)$  share the same poles in  $\text{Re}(s) \geq -\sigma_0$ . To begin Nyquist stability analysis, let  $\sigma_0=0$ . Consider the open-loop transfer function

$$Q(j\omega) \triangleq G_c G G_f(j\omega) \triangleq Q_n(j\omega) + G_c E G_f(j\omega), \quad (4.1)$$

where  $E(j\omega)=G(j\omega)-G_n(j\omega)$ . It is assumed henceforth that  $E(s)$  does not have any poles in  $\text{Re}(s) \geq 0$  since the steady-state response of an unstable pole is unbounded. One can extend this restriction to  $E(s)$

condition that says: all eigenvalues of a system to be shifted by the controller must be included in the model. The problem in applying any of the extended Nyquist stability criteria discussed in §2, arising from such truncation, is that the Nyquist plot of  $Q(s)$  must be known exactly. To overcome this difficulty, Nyquist plots for nonrational transfer functions were obtained using truncated models and bounds on truncation error [Chait 1988a].

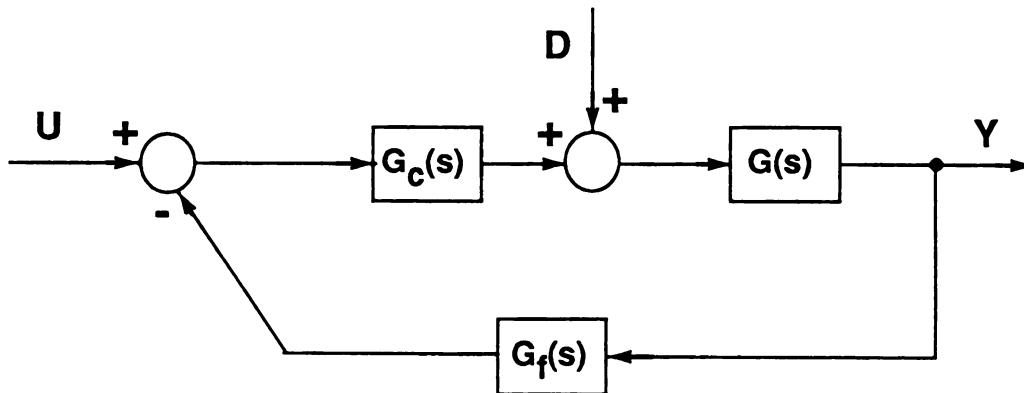


Figure 4.1: The feedback control system including input disturbances

**Lemma 4.1.** The number of encirclements  $(-1,0)$  of the nonrational open-loop system  $Q(s)$  can be determined using a Nyquist plot of the rational open-loop system  $Q_n(s)$  and a tube of uncertainty.

**Proof.** Bounding the truncation error modulus of the open-loop frequency response function gives

$$|Q(j\omega) - Q_n(j\omega)| = |G_c(j\omega)E(\omega)G_f(j\omega)| \leq |G_c G_f(j\omega)R_i|, \quad i=1 \text{ or } 2. \quad (4.2)$$

The tube of uncertainty is defined by the smaller error circle of radius  $|G_c G_f(j\omega)R_i|$  obtained for each point in the range of  $\omega$ . Thus the Nyquist plot of the nonrational  $Q(s)$  can be described by the

Nyquist plot of a rational  $Q_n(s)$  and the tube of uncertainty. Note that this bound is proportional to the gains of  $G_c(j\omega)$  and  $G_f(j\omega)$ .

*Remark 4.2.* In practice, the Nyquist plot can only be computed up to some finite frequency along the imaginary axis, say  $\omega'$ , and an additional bound circle which contains the Nyquist plot of  $Q(\omega)$  for all frequencies higher than  $\omega'$ , must be defined. The radius of this additional bound obtained for equation (8) is

$$R_3(\omega') \triangleq \sup |G_c G_f(j\omega) [G_n(j\omega) + R]|, \quad \omega \in [\omega', \infty). \quad (4.3)$$

When  $R_3(\omega')$  is so large that no stability conclusion can be drawn, then either the order of  $G_n(j\omega)$  or the maximum computed frequency  $\omega'$  must be increased until a conclusion can be drawn. An example for the above condition is whenever  $R_3(\omega')$  is equal to or greater than unity. This is a straight forward test for deciding on the largest frequency  $\omega'$  in the construction of the Nyquist plot.

*Remark 4.3.* Compensators with poles on the imaginary axis rule out the construction of a tube of uncertainty since the radius of the tube in (4.2) is infinity at each of these poles. This problem can be alleviated for certain truncation cases. When  $G_c(s)G_f(s)$  has a pole at  $s=j\omega_0$ , the Nyquist contour is indented to the left about the pole. Clearly, the indentation contour  $\Gamma$  results in an infinite semi-circle Nyquist plot for  $Q(s) = G_c(s)G_f(s)[G_n(s) + E(s)]$ . Let  $M_1$ ,  $M_2$ ,  $\phi_1$ , and  $\phi_2$  be the magnitude and the phase of  $G_c(s)G_f(s)$  and  $[G_n(s) + E(s)]$ , respectively; the magnitude of  $Q(s)$  is  $M_1M_2$  and the phase is  $\phi_1 + \phi_2$ . If  $M_2 > E(s) > 0$ , for  $s \in \Gamma$ , then  $|Q(s)|$  is dominated by  $M_1$  which shows that  $|Q(s)|$  also describes an infinite semi-circle. The complex number  $Q(s)$  at the end points of  $\Gamma$  is within some arc about the complex number  $G_c(s)G_f(s)$ . The angle of the arc is defined by the sector which the

error  $E(s)$  generates about the complex number  $G_n(s)$ , at the end points. Simply stated, when  $M_2 > E(s) > 0$ , then the Nyquist plot of  $Q(s)$  is essentially the same as the Nyquist plot for  $Q_n(s)$ , and hence, there is no need for a tube there. Similar arguments can be used when  $G_c(s)G_f(s)$  has poles close to the imaginary axis which yield unexceptionable large error radii.

*Remark 4.4.* Note that the size of the tube of uncertainty is proportional to the open-loop DC gain,  $K$ , of the compensators  $G_c G_f(s)$ ,

$$G_c G_f(s) = K \frac{(s/z_1+1) \cdots (s+z_m+1)}{(s/p_1+1) \cdots (s/p_n+1)}, \quad (4.4)$$

where  $m \leq n$  and where  $z_i$  and  $p_i$  are real or complex. It is suggested that, whenever this gain  $K$  is greater than unity, both sides of Equation (4.2) should be divided by  $K$ . This division translates to shifting the  $(-1,0)$  point to the  $(-1/K,0)$  point. The advantage is obvious.

#### 4.2. Closed-Loop Stability [Chait 1988a,c]

Suppose that the open-loop system  $Q(s)$  has  $p_0$  poles in the open right-half plane  $\text{Re}(s) > 0$ . Using the extended Nyquist stability criterion from §2 and the error bounds from §3, three cases are distinguished for the nonrational closed-loop system: guaranteed stability, guaranteed instability, and an uncertain case.

- (a) *Whenever the point  $(-1,0)$  is encircled  $p_0$  times in the counterclockwise direction by the tube of uncertainty, then the nonrational closed-loop system is guaranteed to be*



- asymptotically stable when  $\sigma_0=0$  and exponentially stable when  $\sigma_0>0$ .
- (b) Whenever the point  $(-1,0)$  is not encircled  $p_0$  times in the counterclockwise direction by the tube of uncertainty, then the nonrational closed-loop system is guaranteed to have poles in  $\text{Re}(s)>\sigma_0$ .
- (c) Whenever the point  $(-1,0)$  is inside the tube of uncertainty, then stability is an open question.

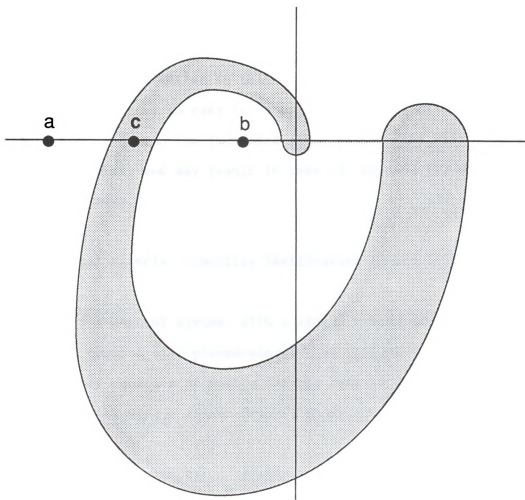


Figure 4.2: The different stability cases of the modified Nyquist criterion - a) guaranteed stability, b) guaranteed instability, and c) undetermined stability



The key point here is that cases (a) and (b) guarantee simultaneous stability or instability for the nonrational system and for the truncated system.

As is the custom, only the polar plot for  $\omega \in (0, \infty)$  is drawn, and the polar plot for  $\omega \in (-\infty, 0]$  is its reflection about the real axis. The above three cases are illustrated in Figure 4.2 where the points *a*, *b*, and *c* represent different locations for the  $(-1, 0)$  point. Assuming an open-loop stable system ( $p_0=0$ ) and  $\sigma_0=0$ , for a closed-loop system to be unstable, it is necessary that the truncated Nyquist plot of  $Q_n(s)$  encircles the  $(-1, 0)$  point. In practice, the compensator is chosen such that  $Q_n(s)$  yields a stable closed-loop system. Thus, the typical problem caused by truncation is that the  $(-1, 0)$  point lies inside the tube of uncertainty as in case (c) where stability is unknown. Retaining more modes in the truncated model reduces the size of the tube of uncertainty and may result in case (a) or case (b) where stability is known.

#### 4.3. Numerical Example: Stability Verification [Chait 1988a]

Consider a control system, with a single sensor and actuator pair, for feedback control of a pinned-pinned beam (Figure 4.3). The Bernoulli-Euler equation of motion for the lateral vibration of a uniform beam including a linear damping model [Chen 1982] is

$$EI \frac{\partial^4 z(x,t)}{\partial x^4} - \nu \frac{\partial^3 z(x,t)}{\partial x \partial t} + m \frac{\partial^2 z(x,t)}{\partial t^2} = a(x) u(t), \quad (4.5)$$

where  $z(x,t)$  is the lateral displacement of an arbitrary point on the beam at any given time  $t$ ,  $EI$  is the bending stiffness,  $\nu$  is a damping

factor,  $m$  is the mass per unit length,  $u(t)$  is the external force amplitude applied to the beam, and  $a(x)$  is the force spatial distribution. The boundary conditions corresponding to pinned ends are

$$z(0,t) = z(L,t) = \frac{\partial^2 z(0,t)}{\partial x^2} = \frac{\partial^2 z(L,t)}{\partial x^2} = 0, \quad (4.6)$$

where  $L$  is the length of the beam. Without loss of generality, the beam parameters  $EI$ ,  $m$ , and  $L$  can be set to unity.

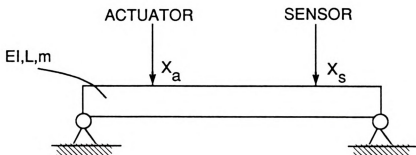


Figure 4.3: The Bernoulli-Euler beam showing the actuator and sensor

The solution of Equations (4.5)-(4.6) can be obtained using the separation of variables method [e.g. Meirovitch 1967] and is given by

$$z(x,t) = \sum_{k=1}^{\infty} \phi_k(x) q_k(t), \quad (4.7)$$

where  $\phi_k(x)$  are the mode shapes and  $q_k(t)$  are the modal amplitudes given by

$$\ddot{q}_k(t) + 2\zeta_k \omega_k \dot{q}_k(t) + \omega_k^2 q_k(t) = u_k(t), \quad k=1,2,\dots, \quad (4.8)$$

where  $\omega_k = (k\pi)^2$  are the mode natural frequencies,  $\phi_k = \sqrt{2}\sin(k\pi x)$  are the orthonormal mode shapes,  $\zeta_k$  are the modal damping factors for underdamped modes with overshoot:  $0 < \epsilon_1 \leq \zeta_k \leq \epsilon_2 < 0.707$ , and  $u_k(t)$  are the modal forces. The modal forces are given by

$$u_k(t) = \int_0^1 \phi_k(x) a(x) u(t) dx \triangleq \alpha_k u(t), \quad k=1,2,\dots, \quad (4.9)$$

The sensor output for position measurement is given by

$$y(t) = \int_0^1 b(x) z(x,t) dx \triangleq \sum_{k=1}^{\infty} \beta_k q_k(t), \quad k=1,2,\dots, \quad (4.10)$$

where  $b(x)$  is the sensor spatial distribution. The Laplace-transformed, nonrational transfer function from the control force amplitude  $U(s)$  to the sensor output  $Y(s)$  can be derived directly from Equations (4.7)-(4.10) and takes the form of Equation (3.9)

$$G(s) = \sum_{k=1}^{\infty} \frac{\alpha_k \beta_k}{s^2 + 2\zeta_k \omega_k s + \omega_k^2}. \quad (4.11)$$

The point actuator is located at  $x_a = 1/7$  so that  $\alpha_k = \sqrt{2}\sin(k\pi/7)$ , and the point sensor is located at  $x_s = 5/7$  so that  $\beta_k = \sqrt{2}\sin(k\pi 5/7)$ .

Experimental data indicates that a conservative range for modal damping is between  $\epsilon_1 = 0.005$  and  $\epsilon_2 = 0.5$  [Breakwell 1983]. Different levels of model truncation are considered. A first-order model with  $n=1$  and  $\zeta_1 = 0.005$  is

$$G_1(s) = \frac{0.6784}{s^2 + 0.0987s + 97.4091}, \quad (4.12)$$

with the error bounds (§3)

$$R_1 = 0.1692 \quad \text{and} \quad R_2(\omega) = 13.18/\omega. \quad (4.13)$$

A second-order model with  $n=2$  and  $\zeta_1=\zeta_2=0.005$  is

$$G_2(s) = G_1(s) + \frac{-1.5245}{s^2 + 0.39478s + 1588.54}, \quad (4.14)$$

with the error bounds

$$R_1=0.0408 \quad \text{and} \quad R_2(\omega)=8.106/\omega. \quad (4.15)$$

An illustration of the construction of the Nyquist plot for  $Q(s)$  using the Nyquist plot of  $Q_n(s)$  and a tube of uncertainty is given, for a control system shown in Figure 4.1 with a proportional controller  $G_c(s)=K$ , a unity negative feedback,  $G_f(s)=1$ , and for  $\sigma_0=0$ . The Nyquist plot of the open-loop system  $G_1(j\omega)$  in (4.12) (up to 12 rad/sec), for  $K=1$ , and the tube of uncertainty using  $R_1$  in (4.13) are shown in Figure 4.4. The tube of uncertainty is indicated by the shaded area. The bound on  $|G_1 G_c(j\omega)|$  for  $\omega > 12$  rad/sec is  $R_3=0.184$ . Because the exterior boundary of the tube of uncertainty does not encircle the point  $(-1,0)$  and the system is open-loop stable ( $p_0=0$ ), we conclude that *the nonrational closed-loop system is guaranteed to be asymptotically stable for  $K=1$* . The condition for stability can be found by varying the gain  $K$  until the  $(-1/K,0)$  point brushes the exterior boundary. For  $0 < K < 2.55$  we have guaranteed asymptotic stability (case a), and for

$K \geq 2.55$  stability is an open question (case c). The later implies that although the Nyquist plot of  $G_1(s)$  never encircles the  $(-1,0)$  point, for any choice of  $K$ , there exists a possibility that higher modes can go unstable for a larger gain  $K$ . This point is now illustrated by retaining more modes in the truncated model.

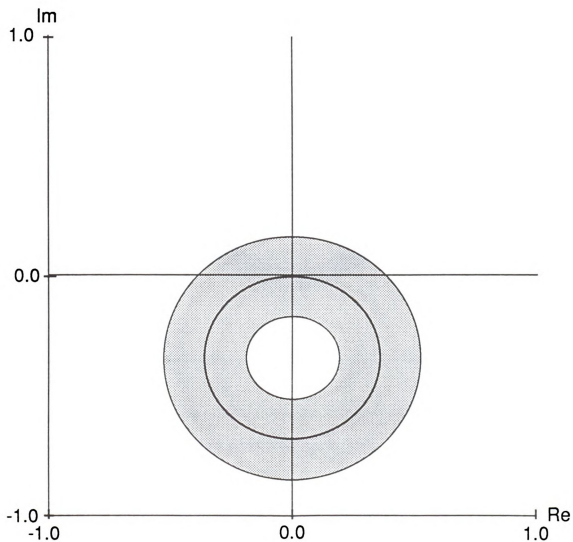


Figure 4.4: Nyquist plot for  $G_c=1$ ,  $n=1$ , and  $x_a=1/7$   $x_s=5/7$

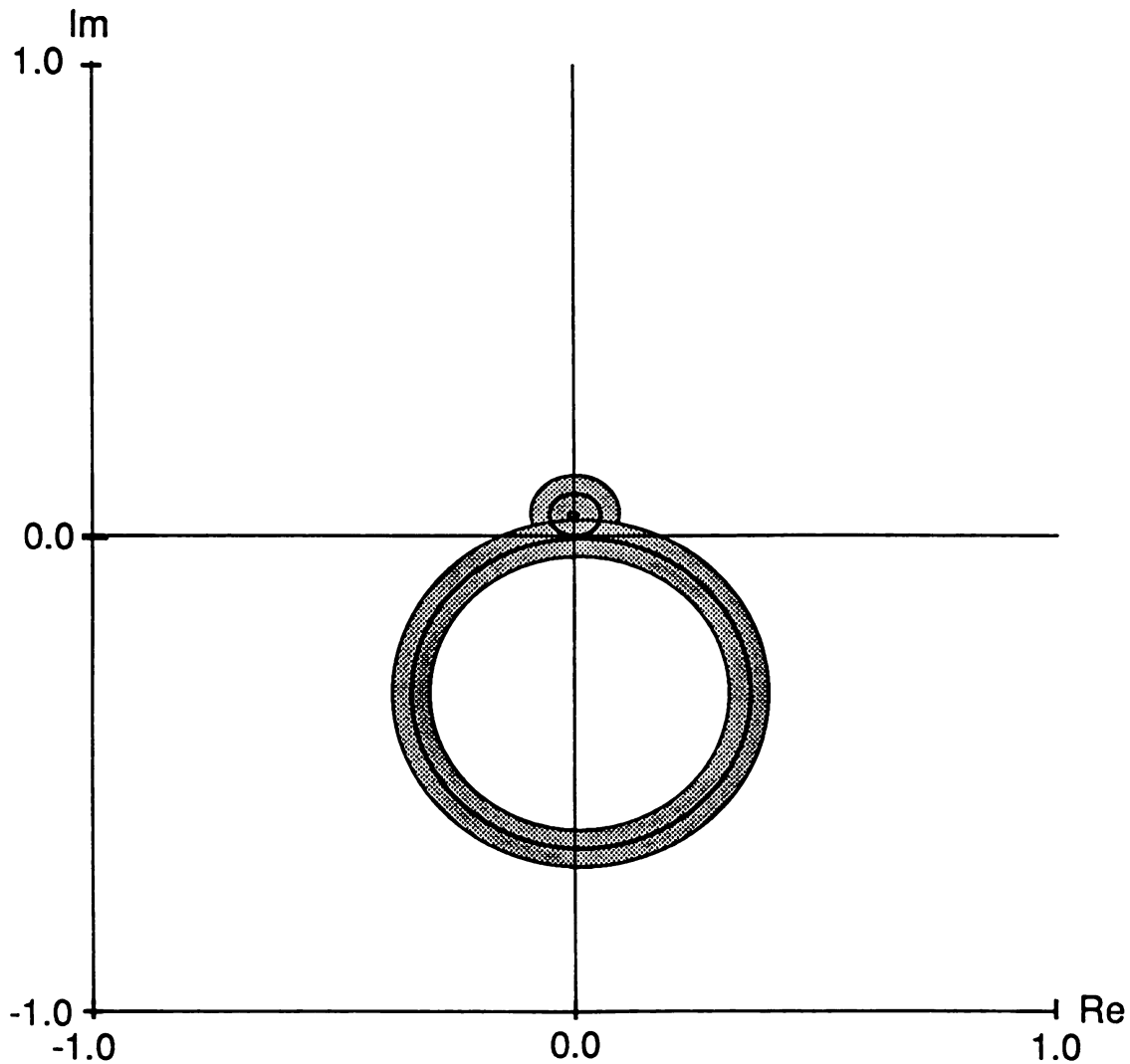


Figure 4.5: Nyquist plot for  $G_c=1$ ,  $n=2$ , and  $x_a=1/7$   $x_s=5/7$

The Nyquist plot of the open-loop system  $G_2(j\omega)$  in (4.14) (up to 42 rad/sec), for  $K=1$ , and the tube of uncertainty using  $R_1$  in (4.15) are shown in Figure 4.5. The bound on  $|G_1G_c(j\omega)|$  for  $\omega>12$  rad/sec is  $R_3=0.05$ . Because the new truncated Nyquist plot crosses the negative real axis as indicated by the tube of uncertainty, it may encircle the

(-1,0) point for some large gain  $K$ . *The nonrational closed-loop system is guaranteed to be asymptotically stable for  $0 < K < 5.62$ . This maximum stable range is larger compared with the previous gain range of  $0 < K < 2.55$  obtained for  $n=1$  only, exactly because  $n=2 > n=1$ . Increasing the number of modes in the truncated model always changes the truncated frequency polar plot as well as the size of the tube of uncertainty, hence refining the evaluation of the range of guaranteed stable or unstable closed-loop gain.*

## §5. CONTROL DESIGN IN THE FREQUENCY DOMAIN

A major objective in control of flexible structures is to suppress vibration caused either by unknown disturbances or by fast maneuvers. A typical feedback control system for this purpose is shown in Figure 4.1. Because the flexible system has an infinite number of modes, and since usually the first few modes dominate the rest of the modes in terms of the system response, the actual design is concerned with improving performance in those few modes only. Closed-loop performance can be measured either by gain and phase margins which are generally related to damping and stability margin or by the closed-loop frequency response magnitude.

The exact location of where the disturbance enters the beam is rarely known, and we will assume it to be at the actuator location  $x_a$ . If some modal amplitude  $\delta_k$  is zero (the  $i$ th eigenfunction has a node at either  $x_a$  or  $x_s$ ), then no controller can dissipate energy at that mode frequency, arising from a disturbance acting at a location where  $\delta_k$  is nonzero. This is known as the controllability-observability issue in control of flexible systems [Simon 1968, Balas 1978]. Therefore, one design constraint is that the actuator and sensor be located such that  $\delta_k \neq 0$  for energy dissipation from that mode.

### 5.1. Design for Improved Damping and Stability Margin [Chait 1988c]

A common and effective controller employed for this purpose is a derivative compensator designed to dissipate energy from the first few



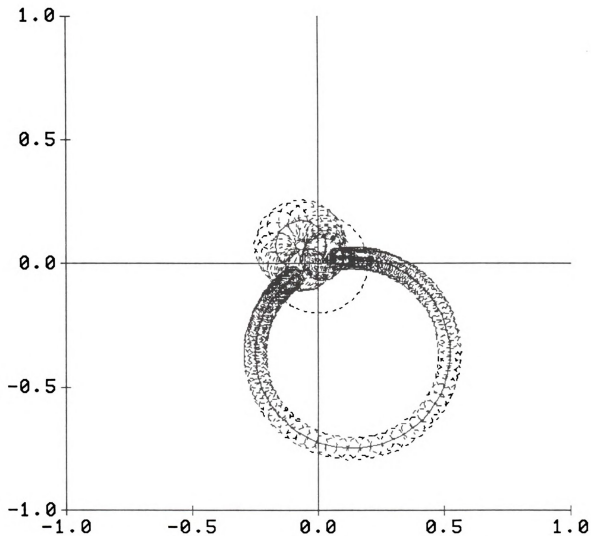


Figure 5.1: Nyquist plot for single lead,  $n=2$ , and  $x_a=1/7$   $x_s=5/7$

vibration modes, and in many cases the first mode only. A physically realizable version of the derivative controller is the lead compensator

$$G_c(s) = K \frac{(Ts+1)}{(aTs+1)}, \quad 0 < a < 1. \quad (5.1)$$

Let  $T=0.05$  and  $a=0.2$ , and let  $G_f(s)=1$ ;  $K=1$  in all the following Nyquist plots. This compensator, for a truncated model with  $n=1$ , can significantly improve the damping ratio of the truncated system (4.12). However, the negative sign in the numerator of the second mode's transfer function (4.14) introduces a pair of nonminimum phase zeros given in  $G_2(s)$ . The dynamic compensator modifies the Nyquist plot for the truncated model (Figure 5.1) by reorienting the plot in a CCW direction. As expected, the plot for the first mode is moved away from  $(-1,0)$ , which indicates increased damping in this mode. However, the tube of uncertainty (4.3) expands in proportion to the increasing magnitude of the lead compensator. The result is that the second mode's plot is both closer to  $(-1,0)$  and has a wider tube, which suggests that both the damping and the stability margin of the second mode are reduced. Guaranteed stability for high compensator gain cannot be achieved because of the reduced stable gain range. The optimal method for constructing a tube of uncertainty from bound circle is yet to be developed. Advanced computer graphics was used in drawing the tube shown in Figures 4.4 and 4.5, however, due to some computational difficulties the tubes in Figures 5.1-5.5 are obtained by drawing each bound circle in the frequency range. Also, the uniform bound on the truncation error was used exclusively in all the plots in this chapter, however, the magnitude of a lead compensator increases with the frequency thus causing an increase in the radii of the bound circles. The result is an increasing in size tube of uncertainty.

When the actuator and sensor are collocated, the nonrational transfer function does not have nonminimum phase zeros [Wie 1981]. However, a noncollocated pair results in nonminimum phase zeros and a truncated model, depending on the order of the truncation, may or may not include any of these zeros. Thus, in a design using truncated

models, both truncation errors and nonminimum phase zeros must be accounted for. The criterion in §4 resolved this problem. Models with these zeros and control design limitations are discussed at length in Cannon (1984).

To increase the lead compensator effectiveness the sensor is moved to  $x_s = 3/7$  which results in a positive modal amplitude  $\delta_2$ . For a truncation with  $n=4$  and  $\zeta_k = 0.005$ ,  $k=1-4$ , the resulting model is

$$G_4(s) = \frac{0.846}{s^2 + 0.0987s + 97.4091} + \frac{0.6784}{s^2 + 0.39478s + 1588.54} + \frac{-1.5245}{s^2 + 0.8883s + 7890.136} + \frac{-1.5245}{s^2 + 1.5791s + 24936.73}, \quad (5.2)$$

with the error bounds

$$R_1 = 0.0075 \quad \text{and} \quad R_2(\omega) = 4.59/\omega. \quad (5.3)$$

Because of both  $\delta_1$  and  $\delta_2$  are positive, the truncated plot for  $n=2$  does not have nonminimum phase zeros and its plot will not cross the real line. The plot for the 3rd and 4th modes does cross the real line since both  $\delta_3$  and  $\delta_4$  are negative since each introduce nonminimum phase zeros to  $G_4(s)$  (5.2).

The physical interpretation is that a positive sign for  $\delta_k$  indicates that the actuator and sensor are in phase at that mode frequency, and negative derivative feedback does actually dissipate energy at that frequency. A negative sign for  $\delta_k$  indicates that energy is being added by the controller to the system at that frequency. These non-minimum phase zeros, which exist in transfer functions of noncollocated systems, **limit** how much energy dissipation can be achieved with any given compensator.

The resulting Nyquist plot for the truncated model in (5.2) has a much smaller tube since  $n=4$  (Figure 5.2). It also crosses the real axis twice with the plots of the 3rd and 4th modes since both  $\delta_3$  and  $\delta_4$  are negative. This crossing can be observed in a detailed Nyquist (Figure 5.3) plot for the 3rd and 4th modes from Figure 5.2. Because the size of the tube is smaller, gain and phase margins become larger, and stability can be guaranteed for a larger gain. Note that in this

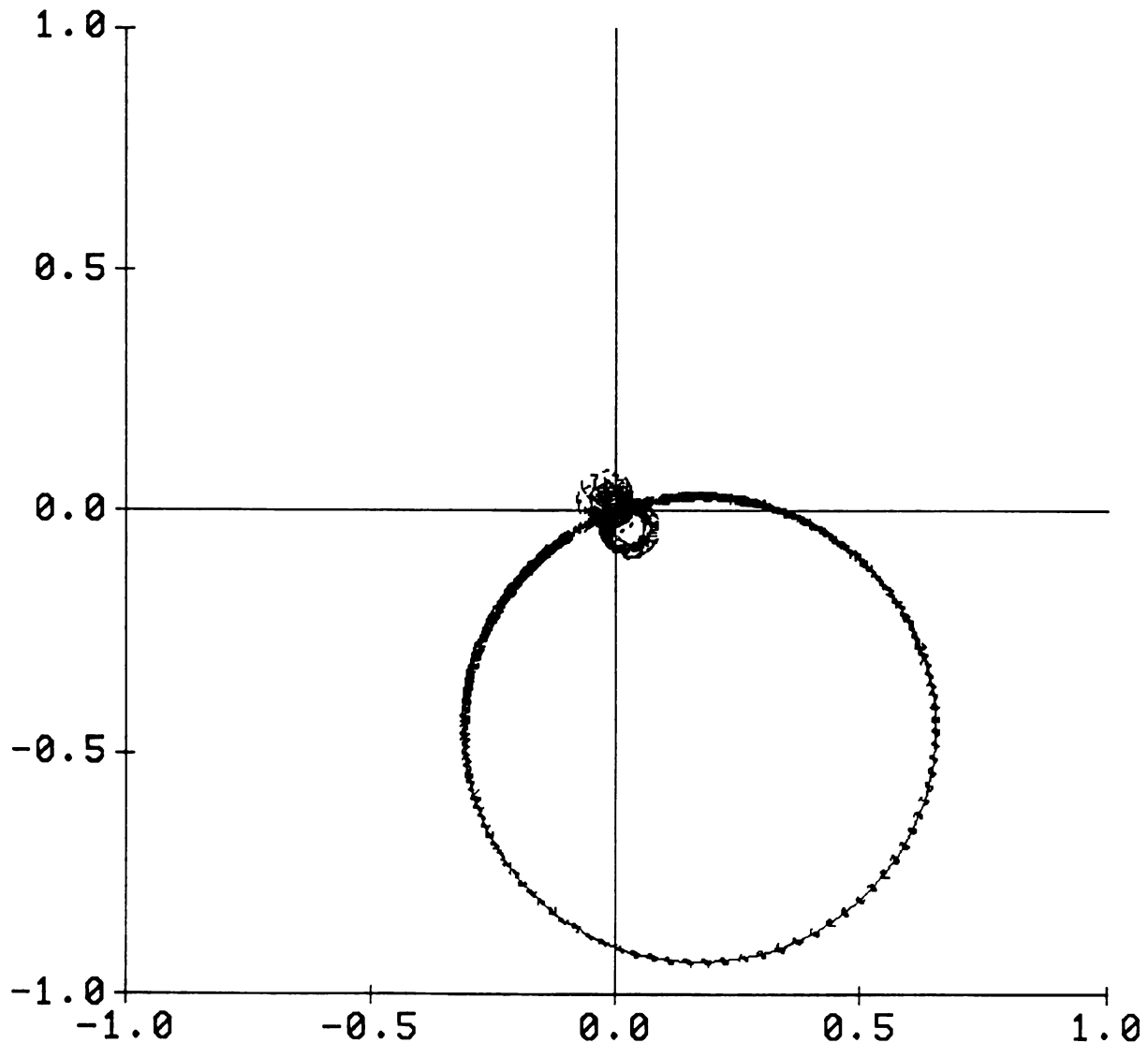


Figure 5.2: Nyquist plot for single lead,  $n=4$ , and  $x_a=1/7$   $x_s=3/7$



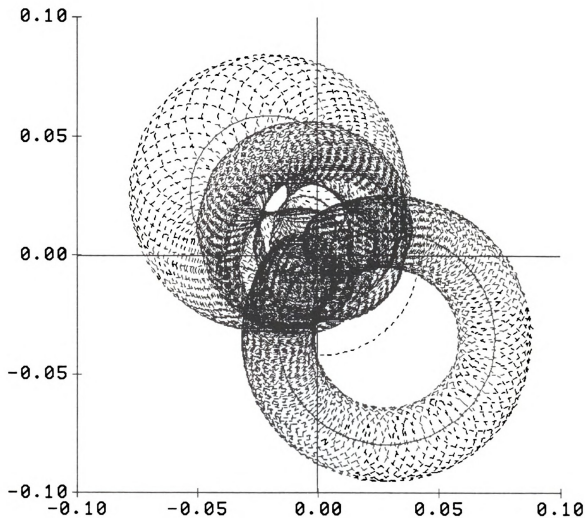


Figure 5.3: Local Nyquist plot of Fig. 5.2

example, the phase margin is undefined since the magnitude is always less than unity.

Higher order compensators should provide more flexibility in the design and result in better closed-loop performance, if designed carefully to consider truncation errors and nonminimum phase zeros via the tube of uncertainty. Consider a double lead compensator



$$G_c(s) = K \frac{(Ts+1)(Ts+1)}{(aTs+1)(aTs+1)}, \quad 0 < a < 1. \quad (5.4)$$

This higher order compensator further reorients the first and second modes' plot away from  $(-1,0)$ , which usually indicates added damping (Figure 5.4). A root locus for a second order compensator (5.4) would

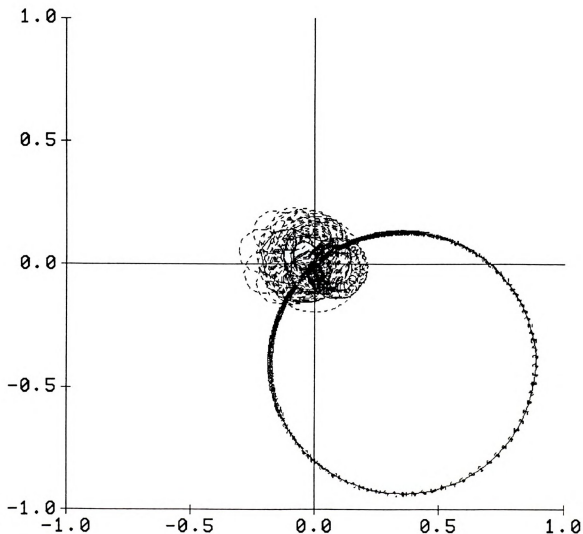


Figure 5.4: Nyquist plot for double lead,  $n=4$ , and  $x_a=1/7$   $x_s=3/7$



show that the closed-loop 1st and 2nd mode poles are shifted further to the left than with a first-order compensator (5.1). However, the 3rd and 4th mode plots are further reoriented toward  $(-1,0)$ , which indicates reduced damping and reduced stability margin. The size of the tube, especially at the 3rd and 4th mode frequencies, is larger than the tube's size for a first-order compensator (5.1). Hence a compromise exists between the order of the compensator and its gain, in order to achieve closed-loop performance.

## 5.2. Closed-Loop Frequency Response Shaping [Chait 1988c]

The nonrational closed-loop frequency response from the disturbance  $D(s)$  to the output  $Y(s)$  (Figure 4.1) is

$$H_n(s) = G_n(s)/[1+Q(s)], \quad (5.5)$$

and the truncated closed-loop transfer function is

$$H_n(s) = G_n(s)/[1+Q_n(s)]. \quad (5.6)$$

Using simple algebra, the closed-loop frequency response error bound is

$$|H(j\omega) - H_n(j\omega)|_\infty \leq |E(\omega)|_\infty / \inf|1+Q(j\omega)| / \inf|1+Q_n(j\omega)|, \quad (5.7)$$

where  $\inf|\cdot|$  is taken along the imaginary axis. These  $\inf|\cdot|$  are readily available from the system's Nyquist plot, where  $\inf|1+Q(j\omega)|$  is equal to the shortest distance between the tube of uncertainty and the point  $(-1,0)$ ; similarly,  $\inf|1+Q_n(j\omega)|$  is equal to the shortest distance between the truncated Nyquist plot and the point  $(-1,0)$ .

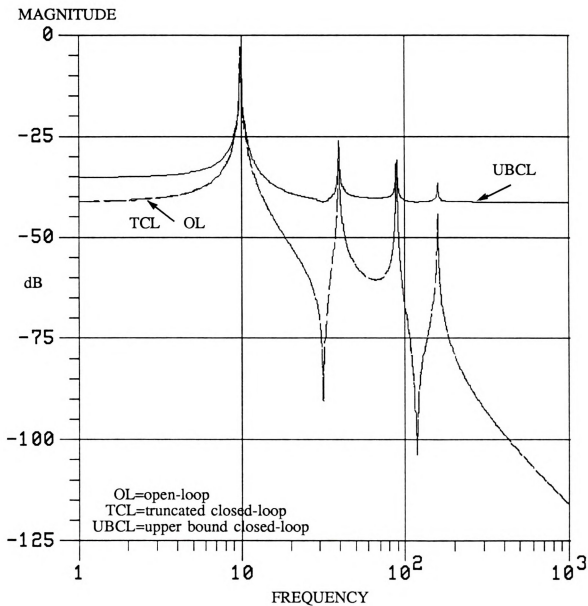


Figure 5.5: Closed-loop frequency response for the system in Fig. 5.2

The truncated closed-loop frequency response magnitude, the upper bound on closed-loop frequency response magnitude, and the open-loop frequency response magnitude approximated by the response of the first 10 modes are compared in order to verify closed-loop performance. This combined plot for  $G_4(s)$  in (5.2) and  $K=1$  is shown in Figure 5.5. The



effectiveness of the lead compensator on the 1st mode magnitude can be observed in Figure 5.6, where the closed-loop frequency function magnitude is reduced from an approximate open-loop value of 0.87 to a guaranteed value, by the upper bound, of 0.65. In this example,  $\inf|1+Q_n(j\omega)|=.939$  and  $\inf|1+Q(j\omega)|=.919$  obtained from Figure 5.2. For

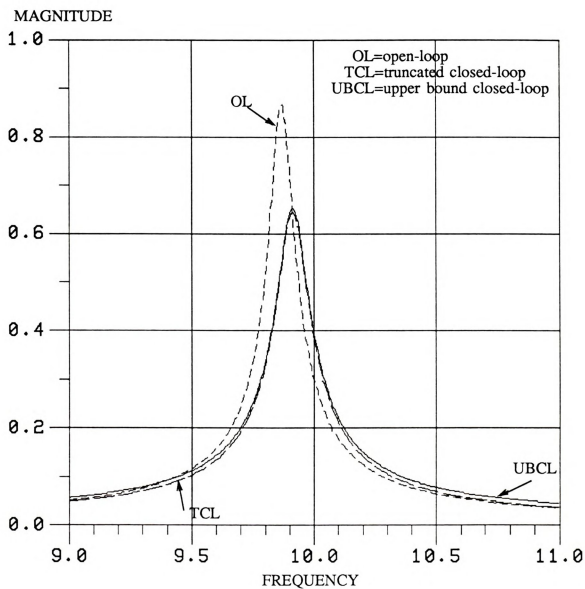


Figure 5.6: Detailed closed-loop frequency response of the 1st mode



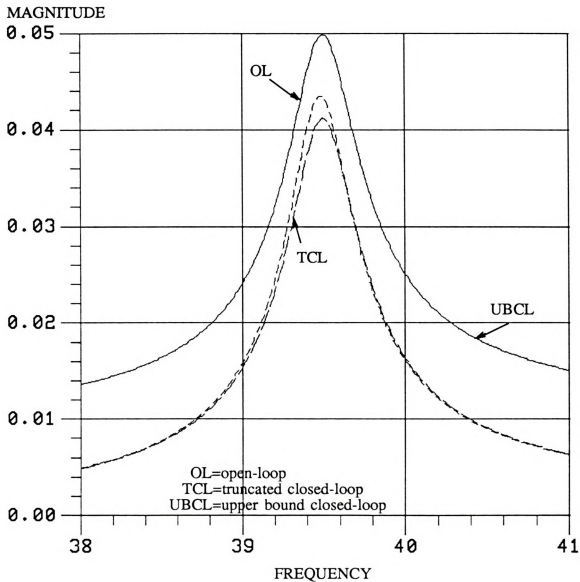


Figure 5.7: Detailed closed-loop frequency response of the 2nd mode

the 2nd mode, the truncated closed-loop frequency response magnitude down to 0.0415 compared with an open-loop magnitude of 0.0428 (Figure 5.7). However, the upper bound magnitude is 0.05, which, in fact, indicates that an increase is also possible. As discussed in the previous section, the 3rd mode's damping factor is reduced, and Figure

5.8 shows an increase from 0.019 to between 0.02 (truncated plot) and 0.029 (upper bound). Using a gain of  $K=2.1$  (Figure 5.9), the 1st mode magnitude is further reduced to between 0.50-0.55. For this case,  $\inf|1+Q_n(j\omega)|=.423$  and  $\inf|1+Q(j\omega)|=.395$  obtained from Figure 5.2.

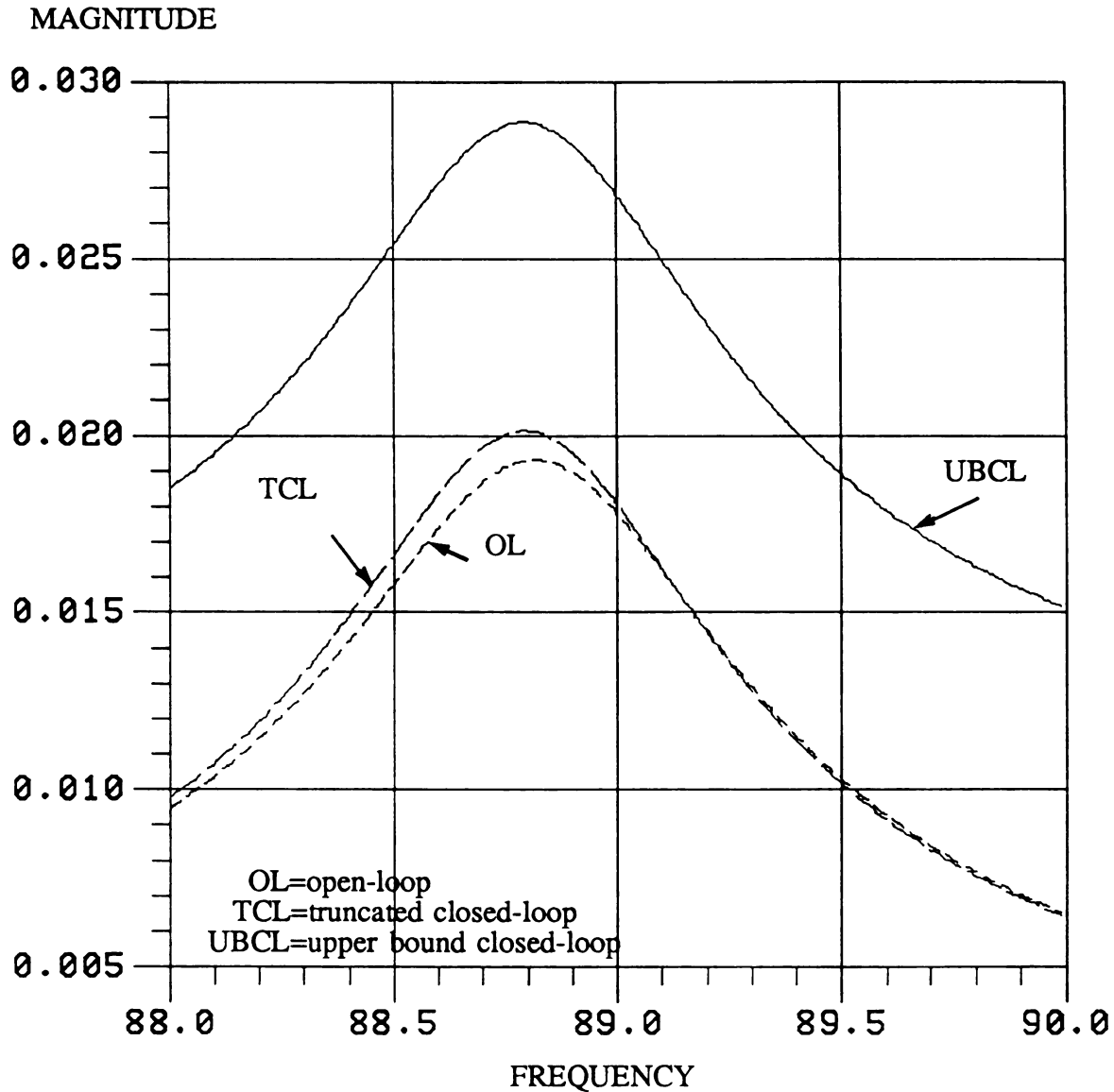


Figure 5.8: Detailed closed-loop frequency response of the 3rd mode

In terms of the 1st mode's magnitude reduction, a double lead compensator (5.4) and gain of  $K=1$ , results in similar magnitude reduction of 0.50 but with a smaller upper bound of 0.51 (Figure 5.10). For this case,  $\inf|1+Q_n(j\omega)|=.743$  and  $\inf|1+Q(j\omega)|=.700$  obtained from Figure 5.4, which is smaller compared with those values in Figure 5.2.

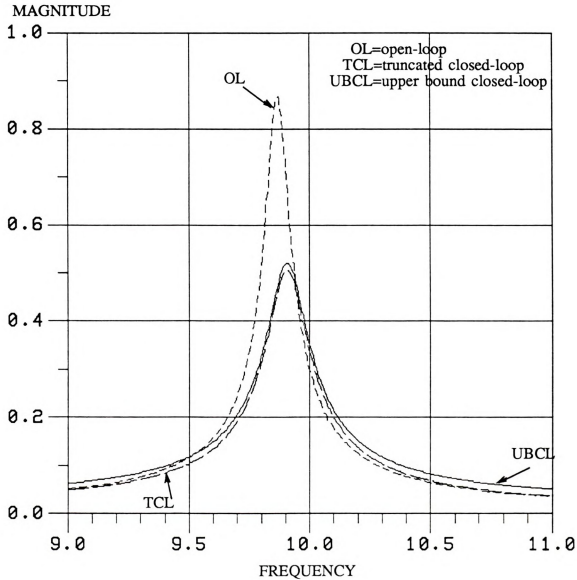


Figure 5.9: 1st vibration mode in Fig. 5.2 and  $K=2.1$

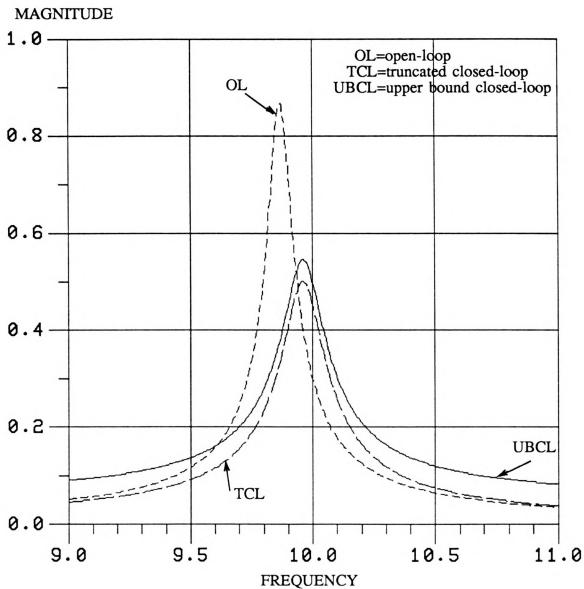
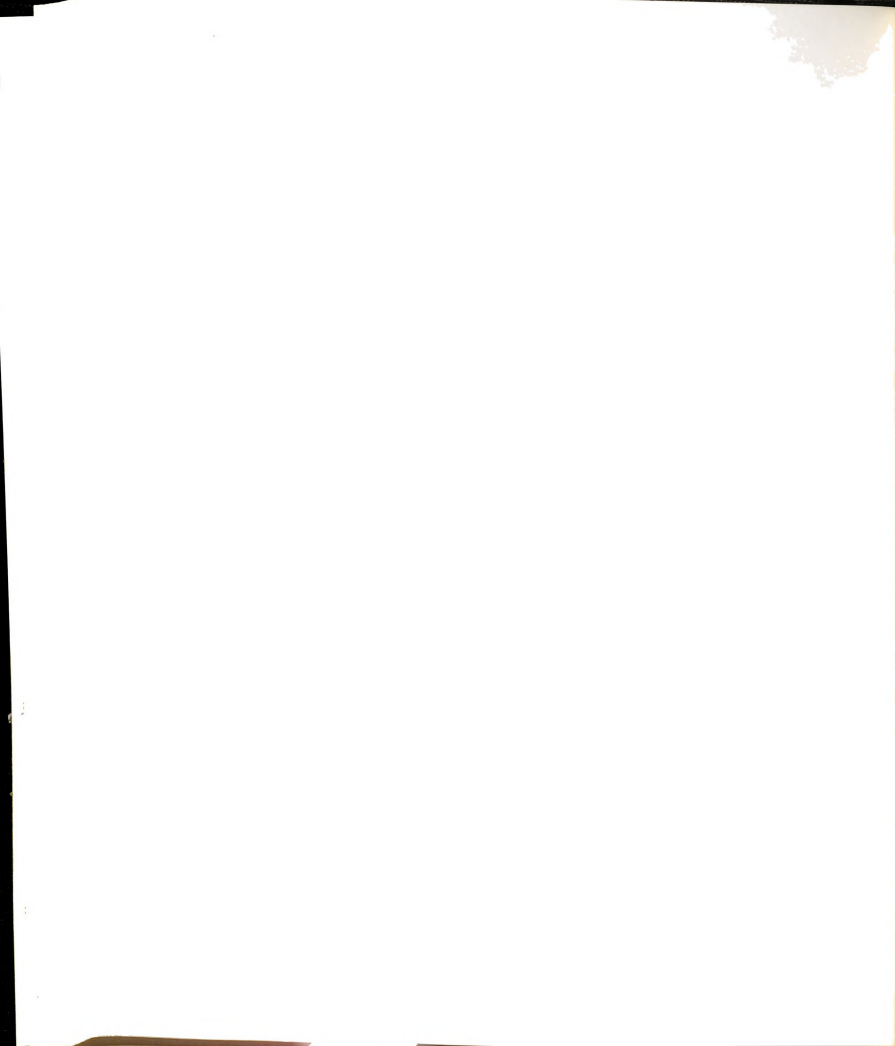


Figure 5.10: 1st vibration mode in Fig. 5.4 5 K-1

This example demonstrate that one has a design choice between a proportional compensator and a double lead compensator for achieving larger closed-loop magnitude reduction in the first mode, and that this method provides a simple tool for evaluating such designs. For both compensator types, this reduction occurs with corresponding response

magnitude increases in higher mode responses. Because higher modes have larger open-loop stability margins than that of the lower modes, this reduction may be acceptable. As control gain is increased further, spillover induced instability may occur as predicted by the previous Nyquist plots.



## CONCLUSIONS

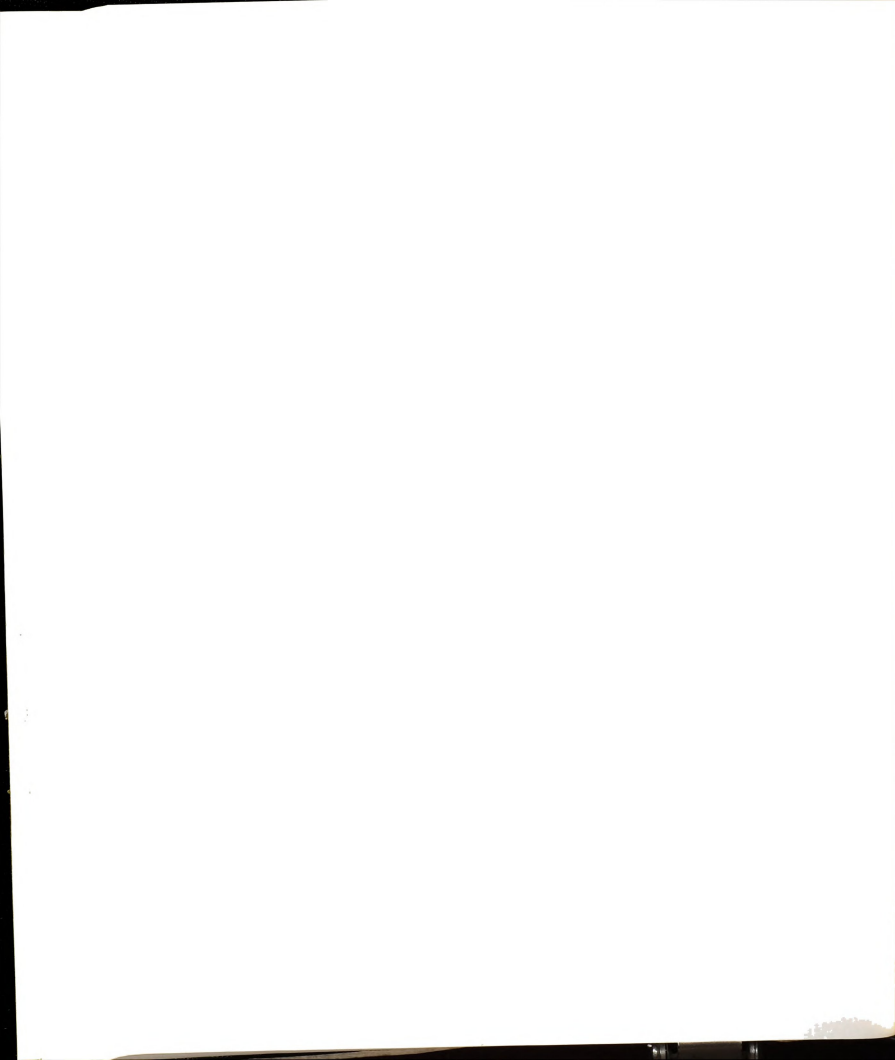
The results of this dissertation addressed the problem of distributed-parameter system control design using truncated models. Results in stability theory and in practical control design are treated in the frequency domain. The results cover DPS whose modal representation is known. The three objectives mentioned on page 7 were met as follows.

i) Model truncation errors and the resulting spillover effects on closed-loop stability can be predicted using our frequency domain stability criterion. The stability is checked using simple graphical tools: a Nyquist plot for a rational model, bounds on truncation errors, and a consequent tube of uncertainty. That stability is guaranteed for the nonrational closed-loop system even though the controller is designed using a truncated model.

ii) The method for computing the truncation error bounds allows for wide uncertainty in the modal damping ratios and in the exact location of the actuator and sensor. The robustness measure for the truncation errors and the above mentioned uncertainties is simply the shortest distance from the tube of uncertainty to the  $(-1,0)$  point on the Nyquist plot.

iii) Classical frequency domain controller design methods for rational transfer function were used. In particular, Nyquist plots and closed-loop magnitude shaping method were employed.

Using the developed theory and the practical design tool the following observations were drawn. Because noncollocated actuator and sensor results in non-minimum phase zeros, compensator gains must be



kept sufficiently low so that higher modes will not be destabilized by the compensator. The numerical examples show that a compromise exists between higher-order compensators and high-gain compensators. Lead compensators were shown to increase damping in the first modes of the beam. However, they also reduced damping in higher modes. The criterion provides a practical stability analysis method to allow compensator design for vibration suppression of the Bernoulli-Euler beam. Associated closed-loop frequency responses with upper bounds predict added damping in some vibration modes and indicate that spillover effects translate into reduced damping in other modes.

In summary, the work done here provides a clear cut indicator for the minimum required number of modes in the truncated model. The controller design process alleviate the need for practical experience, since the robustness measure and the error bounds provide guaranteed results. Similar analysis is possible for any distributed-parameter system with a modal expansion and makes possible controller design for a wide range of engineering systems with guaranteed levels of stability and performance.



## RECOMMENDATIONS FOR FUTURE WORK

Natural future directions are multi input-output and digital version extensions to the theory. The design method could be translated into a user friendly computer program which includes a tube of uncertainty construction such as shown in Figures 4.4-4.5. However, the main trust should be oriented toward developing a conjugate theory to allow for time domain design for DPS using truncated models. In this section we lay out the theoretical basis for such a design. We show that frequency domain open-loop uncertainties, described by a tube of uncertainty, can be utilized to define a corresponding closed-loop system time response uncertainty.

For a system whose closed-loop stability was verified using any of the theorems in §2, we know that the closed-loop transfer function  $H(s)$  is bounded and  $L^1$  on  $\text{Re}(s) \geq -\sigma_0$ , and that its impulse response  $h(t)$  is bounded and  $L^1$  on  $t \in [0, \infty)$ . The following general relations hold for the casual time domain function  $h(t)$  and the frequency domain function  $H(s)$  restricted to  $\text{Re}(s) = -\sigma_0$ , and follows directly from Appendix B:

$$\|h\|_{\infty} \triangleq \sup |h| \leq (1/2\pi) \|H\|_1,$$

and

$$\|h\|_1 \geq \|H\|_{\infty} \triangleq \sup |H|.$$

By the above relations and using the stability result from Section 4.2, having a stable  $H(s)$  implies that the impulse response error  $h(t) - h_n(t)$

is bounded. This is true since  $H(s)$  stable implies  $H_n(s)$  stable under the layout of §2. Such a bound on the impulse response is used in bounding the output error  $y(t) - y_n(t)$  for different classes of inputs.

**Theorem.** Suppose that the control system shown in Figure 4.1 satisfying the hypotheses of Theorem 2.2 is closed-loop stable for some non-negative constant  $\sigma_0$ . In addition, suppose that the input  $U(s)$  is rational, strictly proper, and analytic on  $\text{Re}(s) > 0$  with at most simple poles on  $\text{Re}(s) = 0$ . Then the output error  $y(t) - y_n(t)$  is uniformly bounded when  $\sigma_0 = 0$  and approaches zero exponentially when  $\sigma_0 > 0$ .

**Proof.** The inputs which satisfy the hypothesis can be divided into two classes: (a)  $U(s)$  is analytic on  $\text{Re}(s) > \sigma_1 > 0$  with  $\sigma_1 > 0$ , and (b)  $U(s)$  has simple poles on  $\text{Re}(s) = 0$ . The closed-loop, nonrational, transfer function of the system is

$$Y(s)/U(s) = P(s)/[1+Q(s)] \Delta H(s),$$

and the closed-loop, rational, transfer function of the truncated system is

$$Y_n(s)/U(s) = P_n(s)/[1+Q_n(s)] \Delta H_n(s).$$

By hypothesis,  $H(s)$  and hence  $H_n(s)$  are  $L^1$  on  $\text{Re}(s) \geq -\sigma_0$ , and all  $U(s)$  in class (a) are bounded on  $\text{Re}(s) \geq -\sigma_0$ . Therefore, the inversion formula

$$y(t) - y_n(t) = \int_{-\infty}^{\infty} [H - H_n] U(s) e^{st} ds / 2\pi,$$



is well defined along the vertical line  $\text{Re}(s) = -\sigma$ ,  $\sigma = \min(\sigma_0, \sigma_1)$ .

Bounding terms yields

$$\begin{aligned} \|y(t) - y_n(t)\|_{\infty} &\leq e^{-\sigma t} \int_{-\infty}^{\infty} |[H - H_n]U(j\omega)| d\omega/2\pi \\ &= K e^{-\sigma t}, \quad \sigma = \min(\sigma_0, \sigma_1), \end{aligned}$$

for some constant  $K$ . Using  $\sigma = \min(\sigma_0, \sigma_1)$  instead of  $\sigma_0$  implies that there are no singularities in  $\text{Re}(s) = \sigma_0$  which is required to ensure causality of the time domain functions.

Inputs  $U(s)$  in the class (b) are necessarily bounded in the time domain:  $|u(t)| \leq K_1$ . From Theorem 2.2 we know that  $e^{\sigma_0 t} h(t)$  is  $L^1[0, \infty)$ , and it follows that  $h_n(t)$  has the same property. Using the convolution theorem

$$y(t) - y_n(t) = \int_{-\infty}^{\infty} [H - H_n]U(s) e^{-st} ds/2\pi = e^{-\sigma_0 t} \int_0^{\infty} [h - h_n](t - \tau) u(\tau) d\tau,$$

where  $s = -\sigma_0 + j\omega$ . Bounding terms gives

$$\|y(t) - y_n(t)\| \leq e^{-\sigma_0 t} \|u\|_{\infty} \|h - h_n\|_1 = e^{-\sigma_0 t} K_1 K_2.$$

Note that  $K \leq K_1$ , however, using the Convolution Theorem we take full advantage of  $-\sigma_0$ , where in the first part of the proof we use  $\sigma \leq \sigma_0$ . The reason for requiring input with no unstable poles or repeated poles on the imaginary axis is that such inputs are not bounded in the time domain and hence cannot be produced in real systems



over  $t \in [0, \infty)$ . Having a stable system  $H(s)$  with input  $U(s)$  having poles in the right half plane requires that the inversion integral be evaluated along a vertical line to the right of the furthest pole of  $U(s)$  -- as required for causality of  $y(t)$  -- which contradicts the assumption that  $\sigma_0$  is nonnegative. The strictly proper assumption on  $U(s)$  excludes generalized functions as inputs.

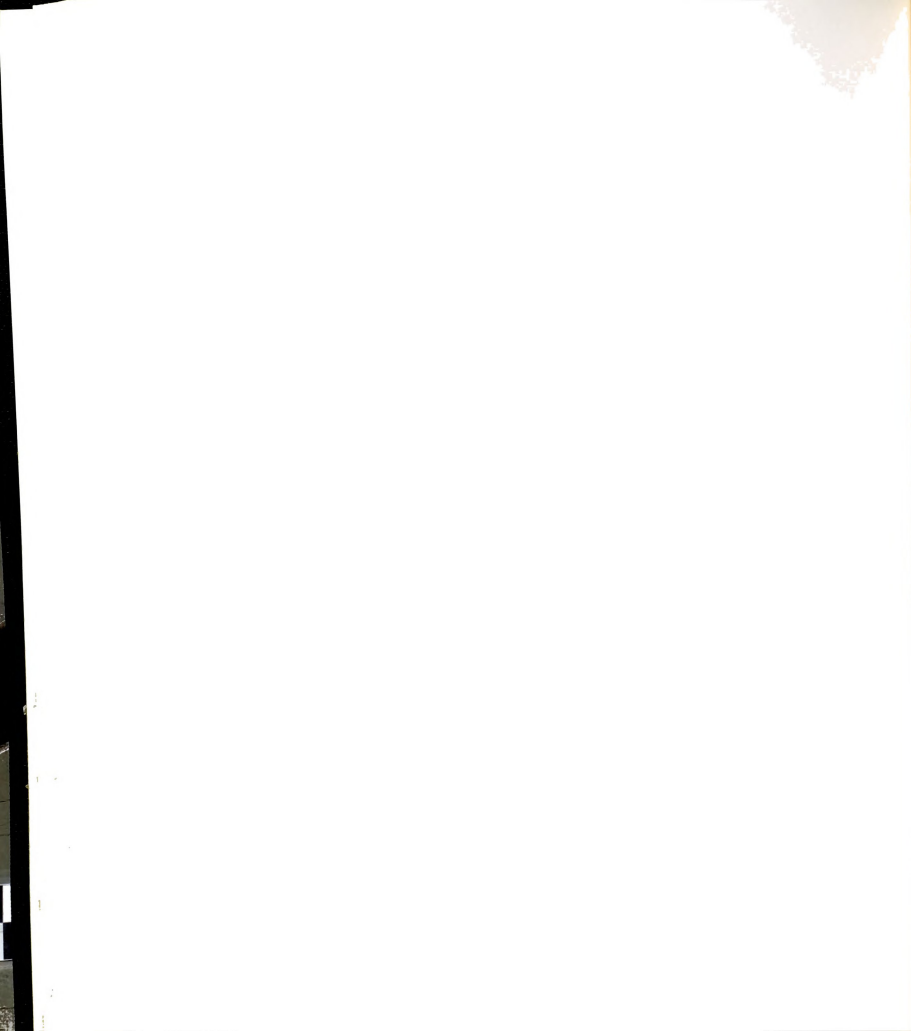
The problem in the application of the above theorem is the difficulty in obtaining a numerical value for  $\|H-H_n\|_1$  and  $\|h-h_n\|_1$ . In some cases, however, it is possible to obtain a numerical value for the norm  $\|H-H_n\|_1$ . Consider the inversion integral for a stable system

$$\int_{-\infty}^{\infty} |[H-H_n]U(-\sigma_0+j\omega)| d\omega = \int_{-\infty}^{\infty} |G_c E U [1+Q]^{-1} [1+Q_n]^{-1}(-\sigma_0+j\omega)| d\omega,$$

where both  $|[1+Q]^{-1}|$  and  $|[1+Q_n]^{-1}|$  are bounded below on the vertical line  $\text{Re}(s)=-\sigma_0$  (from the Nyquist plot). Now suppose that the product  $G_c(s)E(s)$  is  $O(\omega^2)$  on the vertical line  $\text{Re}(s)=-\sigma_0$ , which allows for a numerical evaluation of the integral of  $H(s)-H_n(s)$  over  $(-\infty, -1]$  and  $[1, \infty)$ . Because  $H(s)$  is analytic on  $\text{Re}(s)=-\sigma_0$ , the integral over  $[-1, 1]$  is finite and is given by the bound on the closed-loop frequency response magnitude error (see §5). For example,  $E(s)$  for a second order is  $O(\omega)$ , which combined with a strictly proper  $G_c(s)$  provides the necessary condition for a numerical evaluation.

The Theorem shows that frequency domain tube of uncertainties can be mapped into a time domain tube of uncertainty about the truncated response  $y_n(t)$ . This combined with the results from §2-§5 should provide the control engineer a simple method with absolute guarantee of accuracy for analysis and synthesis of finite-dimensional controllers

for the class of DPS covered in the work, for both frequency domain and time domain specifications.



**APPENDICES**



## APPENDIX A

### Mathematical Preliminaries

**Analytic Function [Hille 1959].** A function  $f(z)$  is said to be analytic (or holomorphic, regular) in a domain  $D$ , if the derivative of  $f(z)$  exists at each point  $z$  of  $D$ . Thus an analytic function is single-valued, continuous, and differentiable in the domain under consideration.

**Meromorphic Function [Hille 1959].** A function  $f(x)$  is said to be meromorphic in a domain  $D$  (finite or extended) if  $f(x)$  is analytic in  $D$  except possibly at singularities which are poles.

**Cauchy Integral Theorem [Hille 1959].** Let  $f(z)$  be analytic in a simply connected domain  $D$ . Let  $C$  be a closed curve within  $D$ . Then

$$\int_C f(z) dz = 0. \quad (A1)$$

**Corollary [Hille 1959].** If  $D$  is simply-connected domain, and if  $a$  and  $b$  are any two points within  $D$ , then

$$\int_a^b f(z) dz \quad (A2)$$

is independent of any continuous path within  $D$  joining  $a$  to  $b$ .



**Cauchy Principal Value of Integrals [Hille 1959].** The improper integral of a continuous  $f(x)$  over the infinite interval  $-\infty \leq x \leq \infty$  is said to be Cauchy P.V. integral

$$\text{P.V.} \int_{-\infty}^{\infty} f(x) dx \triangleq \lim_{R \rightarrow \infty} \int_{-R}^R f(x) dx, \quad (\text{A3})$$

provided this single limit exists. Example: The integral

$$\int_{-\infty}^{\infty} \sin(t) dt \quad (\text{A4})$$

does not exist in the Riemann or Lebesgue sense, however,

$$\text{P.V.} \int_{-\infty}^{\infty} \sin(t) dt = \lim_{R \rightarrow \infty} [-\cos(R) + \cos(-R)] = 0. \quad (\text{A5})$$

**Tonelli's Theorem [Halmos 1950].** If  $h$  is non-negative, measurable function on  $X \times Y$ , then  $\int h d(\nu \times \mu) = \int \int h d\mu d\nu = \int \int h d\nu d\mu$ . In the extended sense, all these integrals are simultaneously infinite, or finite and equal.

**Fubini's Theorem [Halmos 1950].** If  $h$  is an integrable function on  $X \times Y$ , and if the functions  $f$  and  $g$  are defined by  $f(x) = \int h(x, y) d\nu(y)$  and  $g(y) = \int h(x, y) d\mu(x)$ , then  $f$  and  $g$  exist a.e. and are integrable and  $\int h d(\nu, \mu) = \int f d\mu = \int g d\nu$ .

**Jordan Lemma [Papoulis 1962].** If  $t < 0$  and  $f(z) \rightarrow 0$  with  $|z| \rightarrow \infty$ , then



$$\int_{\Gamma} e^{tz} f(z) dz \rightarrow 0 \quad \text{as } r \rightarrow \infty, \quad (\text{A6})$$

where  $\Gamma$  denotes the semicircle  $s = -\sigma_0 + re^{j\theta}$ ,  $-\pi/2 \leq \theta \leq \pi/2$ .

**Lebesgue Bounded Convergence Theorem [Halmos 1950].** If  $\{f_n\}$  is a sequence of integrable functions which converges in measure to  $f$  or else converge to  $f$  a.e. (almost everywhere), and if  $g$  is an integrable function such that  $|f_n(x)| \leq |g(x)|$  a.e.,  $n=1,2,\dots$ , then  $f$  is integrable and the sequence  $\{f_n\}$  convergence to  $f$  in the mean (i.e.,  $\int |f_n - f| dx \rightarrow 0$  as  $n \rightarrow \infty$ ).

*Corollary.*

$$\lim_{y \rightarrow y_0} \int f(x,y) d\nu = \int \lim_{y \rightarrow y_0} f(x,y) d\nu \quad (\text{A7})$$

provided: a)  $\lim[f(x,y)]$  exists for a.e.  $x$  as  $y \rightarrow y_0$ , and

b)  $|f(x,y)| \leq g(x)$ , for some integrable  $g$ .

*Corollary.* Suppose  $|f(x,y)| \leq g(x)$  on  $X$  where  $g(x)$  is absolutely integrable on  $X$ . If  $f(x,y)$  is continuous at  $y_0$  for a.e.  $x$ , then

$$F(y) = \int f(x,y) d\nu(x) \quad (\text{A8})$$

is continuous at  $y_0$ .

**Argument Principle [Hille 1959].** Let  $C$  be a simple closed continuous curve, and let  $f(z)$  be meromorphic inside  $C$  and continuous on  $C$ . When  $z$  describes  $C$  in the clockwise direction, the argument of  $f(z)$  increases by a multiple of  $2\pi$ , namely



$$\arg[f(z)] \Big|_C = 2\pi (Z-P), \quad (\text{A9})$$

where  $Z$  is the number of zeros of  $f(z)$  inside  $C$ , and  $P$  is the number of poles of  $f(z)$  inside  $C$ .

**Nyquist Criterion [Nyquist 1932].** Let  $P(s)$  denote the open-loop rational function (transfer function) in  $s$  and let  $H(s)=P(s)/[1+P(s)]$  be the closed-loop transfer function (which is also a rational function in  $s$ ). Let  $\Gamma$  denote the Nyquist contour that passes along the  $j\omega$ -axis from  $-j\infty$  to  $+j\omega$  and then along the semicircle  $s=re^{j\theta}$ ,  $r\rightarrow\infty$  and  $\theta$  starts at  $\pi/2$  and ends at  $-\pi/2$ , and let  $\Gamma_p$  be the contour generated by  $P(s)$  as  $s$  describes  $\Gamma$ . The closed-loop function  $H(s)$  is exponentially stable if and only if, for the contour  $\Gamma_p$ , the number of counterclockwise encirclements of the  $(-1,0)$  point is equal to the number of poles of  $P(s)$  with positive real part. The proof for this criterion as well as treatment of special cases can be found in many standard control text books, and is a direct consequence of the Argument Principle.

**Riemann-Lebesgue Lemma [Doetsch 1974].** If a function  $f(\omega)$  is absolutely integrable in an interval  $[a,b]$ , then

$$\lim_{t \rightarrow \pm\infty} \int_a^b f(\omega) e^{-j\omega t} d\omega = 0, \quad (\text{A10})$$

where  $a$  and  $b$  are finite constants. In fact, the theorem holds when  $a$  and  $b$  are infinite.

We give here a short proof [Tolstov 1962], based on the following lemma.



**Lemma.** Suppose  $f(\omega)$  is  $L^1$ , then for any  $\epsilon > 0$ , there exists a continuously differentiable function  $p(\omega)$  such that  $\int |f(\omega) - p(\omega)| d\omega < \epsilon$ .

**Proof of the RL Lemma.** Let  $\epsilon > 0$  be arbitrary number, and consider the expression

$$\left| \int_a^b f(\omega) e^{j\omega t} d\omega \right| \leq \int_a^b |f(\omega) - p(\omega)| d\omega + \left| \int_a^b p(\omega) e^{j\omega t} d\omega \right|. \quad (A11)$$

Integrating by parts, we obtain

$$\int_a^b p(\omega) e^{j\omega t} d\omega = (jt)^{-1} [p(\omega) e^{j\omega t}] \Big|_a^b - (jt)^{-1} \int_a^b p'(\omega) e^{j\omega t} d\omega \quad (A12)$$

where  $p'(\omega)$  denotes the derivative. Since  $p(\omega)$  is continuously differentiable the expression in the brackets and the integral are bounded. Therefore, for sufficiently large  $t$

$$\left| \int_a^b p(\omega) e^{j\omega t} d\omega \right| < \epsilon/2. \quad (A13)$$

By the lemma and (A13), it follows that

$$\left| \int_a^b f(\omega) e^{j\omega t} d\omega \right| < \epsilon \quad (A14)$$

for sufficiently large  $t$ , i.e.,

$$\lim_{t \rightarrow \infty} \int_a^b f(\omega) e^{j\omega t} d\omega = 0.$$



*Remark.* The application here to our work is the simple deduction that a time domain response

$$f(t) = \int_{-\infty}^{\infty} F(j\omega) e^{j\omega t} d\omega/2\pi, \quad (\text{A15})$$

vanishes at  $\infty$  when  $F(j\omega)$  is absolutely integrable.

**Asymptotic Stability [Russell 1979].** The linear homogeneous system

$$\dot{x}(t) = Ax(t), \quad x(t_0) = x_0, \quad (\text{A16})$$

$x$  in some Banach space  $X$ , is said to be asymptotically stable if every solution of (A16) satisfies

$$\lim_{t \rightarrow \infty} \|x(t)\| = 0 \quad \text{as } t \rightarrow \infty. \quad (\text{A17})$$

**Bounded-Input Bounded-Output (BIBO) Stability.** The forced linear system

$$\dot{x}(t) = Ax(t) + Bu(t), \quad x(t_0) = x_0, \quad (\text{A18})$$

$x$  in some Banach space  $X$ , is said to be BIBO stable if

$$\|x(t)\| \leq K \|u(t)\|, \quad (\text{A19})$$

for some constant  $K$  independent of  $u$ .



**Exponential Stability.** The linear system (A16) is said to be exponentially stable if

$$\|x(t)\| \leq K e^{-\sigma t}, \quad (\text{A20})$$

for some nonnegative constants  $K$  and  $\sigma > 0$ .



## APPENDIX B

### The Laplace Transform Pair

The Laplace Transform  $F(s)$  of a time-domain function  $f(t)$  is evaluated from the integral

$$\int_0^{\infty} f(t) e^{-st} dt, \quad (B1)$$

where  $s=\sigma+j\omega$ . The conditions for existence of the integral and other properties of  $F(s)$  evaluated by (B1) are presented in the following theorem.

**Theorem B1.** Suppose that  $f(t)e^{-\sigma_0 t}$  is  $L^1[0, \infty)$ ,  $\sigma_0$  real. Then

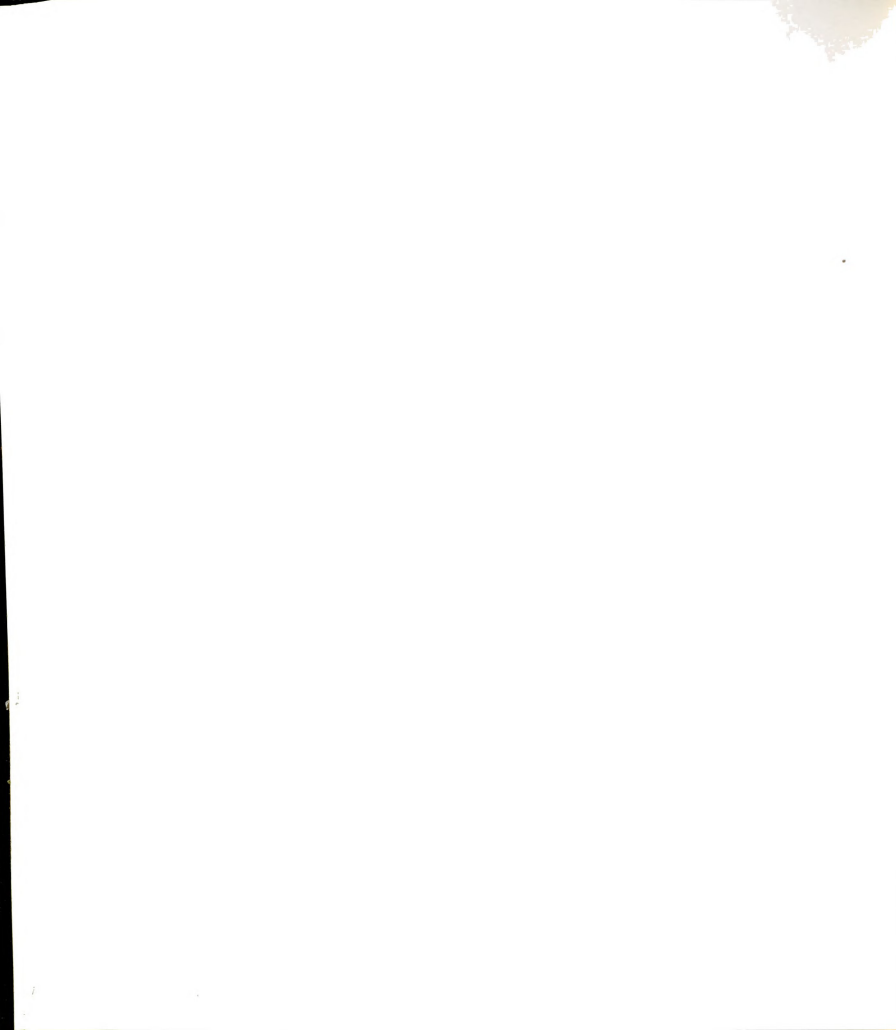
- (a)  $F(s)$  exist for  $\text{Re}(s) \geq \sigma_0$ ;
- (b)  $F(s)$  is bounded in  $\text{Re}(s) \geq \sigma_0$ ;
- (c)  $F(s)$  is uniformly continuous in  $\text{Re}(s) \geq \sigma_0$ ;
- (d)  $F(s)$  is analytic for  $\text{Re}(s) > \sigma_0$ ;
- (e)  $F(s) \rightarrow 0$ , for each in  $\sigma \geq \sigma_0$  as  $\omega \rightarrow \pm\infty$ ;

**Proof.** (a) By hypothesis, the integral (B1) exist for  $s=\sigma+j\omega$  and  $\sigma \geq \sigma_0$ .

(b)

$$|F(s)| = \left| \int_0^{\infty} f(t) e^{-st} dt \right| \leq \int_0^{\infty} |f(t) e^{-\sigma_0 t}| dt < \infty. \quad (B2)$$

(c) Let  $s_0 = \sigma_0 + j\omega$ . By definition,



$$\lim_{s \rightarrow s_0} [F(s) - F(s_0)] = \lim_{s \rightarrow s_0} \int_0^{\infty} f(t) (e^{-st} - e^{-s_0 t}) dt, \quad (B3)$$

where  $s \rightarrow s_0$  in any direction within the half-plane  $\text{Re}(s_0) \geq \sigma_0$ . Because  $f(t) (e^{-st} - e^{-s_0 t}) = f(t) e^{-\sigma_0 t} [e^{-j\omega t} (e^{-(\sigma - \sigma_0)t} - 1)]$ ,  $f(t) e^{-\sigma_0 t}$  is  $L^1$ , and  $|[e^{-j\omega t} (e^{-(\sigma - \sigma_0)t} - 1)]| \leq 1 \forall t_0$ , then by Lebesgue Bounded Convergence Theorem [App. A]  $\lim[f(s_0) - f(s)] = 0$  as  $s \rightarrow s_0$ ,  $\forall \sigma \geq \sigma_0$ .

(d) It suffices to verify that the derivative of  $F(s)$ ,

$$\lim_{s \rightarrow s_0} \frac{F(s) - F(s_0)}{s - s_0} = \lim_{s \rightarrow s_0} \int_0^{\infty} f(t) [(e^{-st} - e^{-s_0 t}) / (s - s_0)] dt \quad (B4)$$

exist  $\forall \sigma > \sigma_0$ , where  $s_0 \rightarrow s$  in any direction in the half-plane  $\text{Re}(s_0) \geq \sigma_0$ ,  $\sigma_0 > -\infty$ . Because  $|[e^{-j\omega t} (e^{-(\sigma - \sigma_0)t} - 1) / (s - s_0)]| \leq 1 \forall t$  and  $f(t) e^{-\sigma_0 t}$  is  $L^1$ , then by the Lebesgue Bounded Convergence Theorem [App. A] the limit exist.

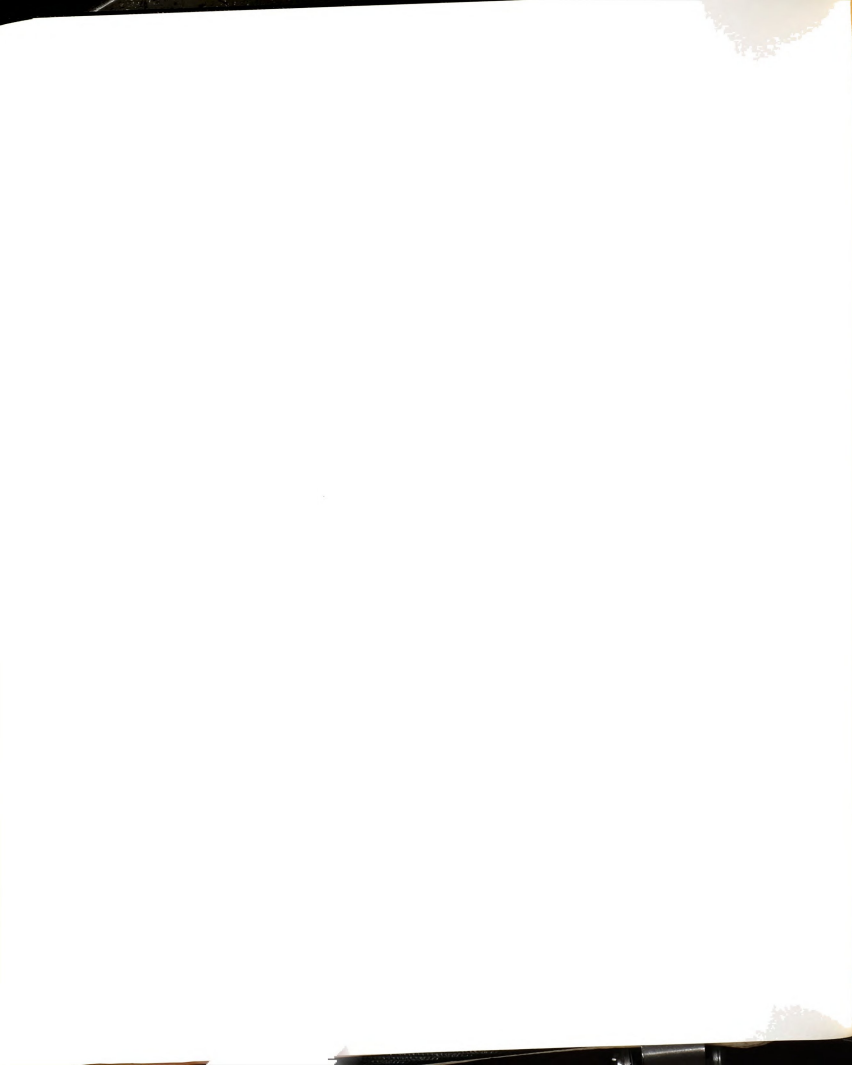
(e) Let  $s = \sigma + j\omega$ , and  $\sigma \geq \sigma_0$ . By hypothesis, for every given  $\epsilon > 0$ , there exist  $T$  such that

$$\left| \int_T^{\infty} f(t) e^{-st} dt \right| \leq \int_T^{\infty} |f(t)| e^{-\sigma t} dt \leq \int_T^{\infty} |f(t)| e^{-\sigma_0 t} dt < \epsilon/2. \quad (B5)$$

By the Riemann-Lebesgue Lemma, there exist  $\Omega$  such that

$$\left| \int_0^T f(t) e^{-st} dt \right| \leq \epsilon/2 \quad \text{for } |\omega| > \Omega, \quad \text{for each } \sigma \geq \sigma_0. \quad (B6)$$

Hence,



$$|F(s)| = \left| \int_0^{\infty} f(t) e^{-st} dt \right| \leq \epsilon \quad \text{for } |\omega| > \Omega. \quad (\text{B7})$$

We now turn to checking whether the time domain function  $f(t)$  can be recovered from its Laplace Transform  $F(s)$  via the inversion integral

$$\int_{\sigma-j\infty}^{\sigma+j\infty} F(s) e^{st} ds/2\pi j = e^{\sigma t} \int_{-\infty}^{\infty} F(\sigma+j\omega) e^{j\omega t} d\omega/2\pi. \quad (\text{B8})$$

**Theorem B2.** Suppose that  $f(t)e^{\sigma_0 t}$  is  $L^1[0, \infty)$  and  $F(s)$  is defined by (B2). Then for each  $\sigma \geq \sigma_0$

$$\text{P.V.} \int_{\sigma-j\infty}^{\sigma+j\infty} F(s) e^{st_0} ds/2\pi j = f(t_0), \quad (\text{B9})$$

at each  $t_0$  where  $[f(t)-f(t_0)]/(t-t_0)$  is integrable near  $t_0$  (Dini's test).

**Proof.** Assume  $\sigma=0$  since this proves the rule. Consider the integral

$$\int_{-\Omega}^{\Omega} F(j\omega) e^{j\omega t_0} d\omega = \int_{-\Omega}^{\Omega} \int_0^{\infty} f(t) e^{-j\omega t} dt e^{j\omega t_0} d\omega, \quad (\text{B10})$$

where  $\Omega$  is a fixed positive constant. Because  $f(t)$  is  $L^1$  on  $t \in [0, \infty)$  and the interval  $[-\Omega, \Omega]$  is compact, then the integrated integral converges absolutely. By Tonneli's Theorem [App. A], the double

integral of  $f(t)e^{-j(\omega-\omega_0)t}$  is absolutely integrable on  $[-\Omega, \Omega] \times [0, \infty)$ .

By Fubini's Theorem [App. A], both iterated integrals converge and are equal, and the integral on the right in (B10) can be written as

$$\int_0^{\infty} f(t) \int_{-\Omega}^{\Omega} e^{-j(t-t_0)\omega} d\omega dt. \quad (\text{B11})$$

which can be reduced to

$$2 \int_0^{\infty} f(t) \sin[(t-t_0)\Omega]/(t-t_0) dt. \quad (\text{B12})$$

But (B12) can be written as the sum of three integrals

$$\begin{aligned} & 2f(t_0) \int_0^T \sin[(t-t_0)\Omega]/(t-t_0) dt \\ & + 2 \int_0^T \{ [f(t)-f(t_0)]/(t-t_0) \} \sin[(t-t_0)\Omega] dt \\ & + 2 \int_T^{\infty} f(t) \{ \sin[(t-t_0)\Omega]/(t-t_0) \} dt, \end{aligned} \quad (\text{B13})$$

for  $T > t_0$ . As  $\Omega \rightarrow \infty$ , the first integral approaches  $2\pi f(t_0)$  because

$$\int_0^T \sin[(t-t_0)\Omega]/(t-t_0) dt = \int_{-\Omega t_0}^{\Omega(T-t_0)} \sin(x)/x dx \rightarrow \int_{-\infty}^{\infty} \text{sinc}(x) dx = \pi. \quad (\text{B14})$$



The second integral tend to zero as  $\Omega \rightarrow \infty$  by the Riemann-Lebesgue Lemma [App. A], since by Dini's assumption  $[f(t)-f(t_0)]/(t-t_0)$  is  $L^1$ . The third integral can be made arbitrarily small for all large  $T$  since  $f(t)$  is  $L^1$  and  $\sin[(t-t_0)\Omega]/(t-t_0)$  is bounded.

A weaker theorem showing when  $f(t)$  can be recovered from  $F(s)$  is presented next.

**Theorem B3.** Suppose that  $F(s)$  is analytic in the half-plane  $\text{Re}(s) > \sigma_1$ ,  $F(s)$  vanishes in every half-plane  $\text{Re}(s) \geq \sigma_1 + \delta > \sigma_1$  as  $s$  tends two dimensionally toward  $\infty$ , and  $F(s)$  is  $L^1$  on every vertical line  $\text{Re}(s) > \sigma_1$ . Then  $F(s)$  is equal to the Laplace Transform (B1) of its original function, which is evaluated with (B2) independent of the choice of  $\sigma$  in  $\sigma > \sigma_1$ .

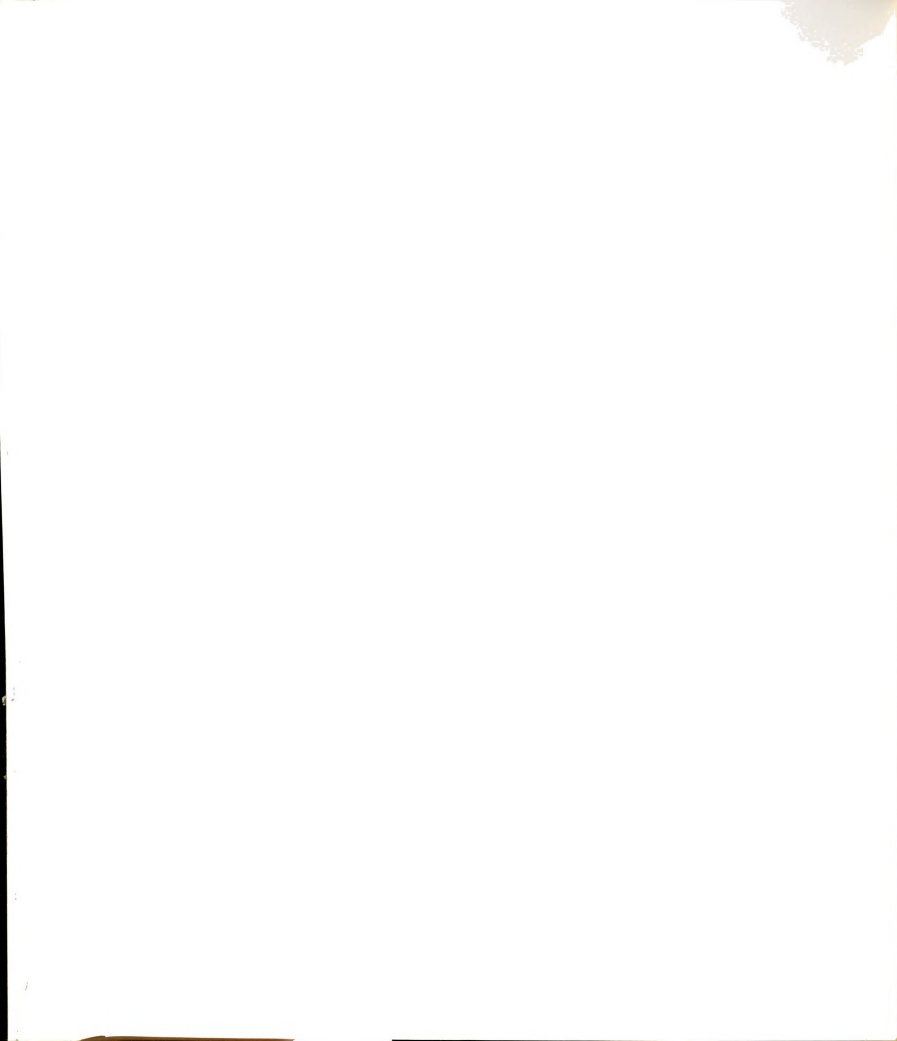
**Proof.** The proof is given in Doetsch (1962).

Let us now turn the process around. Suppose we are given a frequency domain function  $F(s)$  and wish to discover when this  $F(s)$  is in fact the Laplace Transform of a time domain function  $f(t)$ . The answer in general is difficult, deep, and unresolved (see MacCluer 1988). A partial answer follows.

**Theorem B4.** Suppose that

- (i)  $F(s)$  is analytic on  $\text{Re}(s) > \sigma_0$  and continuous on  $\text{Re}(s) \geq \sigma_0$ ;
- (ii)  $F(s)$  is  $L^1$  on  $\text{Re}(s) = \sigma_0$ ;
- (iii)  $F(s)$  is strictly proper on  $\text{Re}(s) \geq \sigma_0$ .

Then



- (a)  $f(t)$  is well defined by (B8) independent of  $\sigma$  for  $\sigma \geq \sigma_0$ ,
- (b)  $f(t)$  is bounded on  $[0, \infty)$ ,
- (c)  $f(t)$  is uniformly continuous on  $[0, \infty)$ ,
- (d)  $f(t) = O(e^{\sigma_0 t})$ ,
- (e)  $f(t)$  is causal, and
- (f)  $f(t) \rightarrow 0$  as  $t \rightarrow \infty$ .

**Proof.** (a) Using hypotheses (ii) and (iii), the result follows by the Cauchy Integral Theorem [App. A].

(b) By hypothesis, the integral (B8) exist as  $L^1$ , hence  $f(t)$  is bounded.

(c) Continuity follows from the Lebesgue Bounded Convergence Theorem [App. A] (see the proof given for Thm. B1 part 3).

(d) Because  $F(s)$  is  $L^1$  on  $\text{Re}(s) = \sigma_0$

$$f(t) \ll e^{\sigma_0 t} \int_{-\infty}^{\infty} |F(\sigma_0 + j\omega)| d\omega / 2\pi, \quad (\text{B15})$$

giving  $f(t) = O(e^{\sigma_0 t})$ .

(e) Because  $F(s)$  is analytic on  $\text{Re}(s) > \sigma_0$  and continuous on  $\text{Re}(s) = \sigma_0$ , by the Cauchy Integral Theorem [App. A] the integral (B8) can be separated into five contour integrals by breaking the contour  $\Gamma$  into five contours

$$\Gamma = \Gamma_1 + \Gamma_2 + \Gamma_3 - \Gamma_2^* - \Gamma_1^*, \quad (\text{B16})$$

where on  $\Gamma_1$   $s = \sigma_0 + j\omega$ ,  $\omega \in (-\infty, -\Omega)$  for  $\Omega$  a large positive constant, on  $\Gamma_2$   $s = \sigma - j\Omega$ ,  $\sigma \in [\sigma_0, \sigma_1]$  for  $\sigma_1 > \sigma_0$ , on  $\Gamma_3$   $s = \sigma_1 + j\omega$ ,  $\omega \in [-\Omega, \Omega]$ , and where  $(\cdot)^*$

denotes the complex conjugate. Because  $F(-\sigma_0+j\Omega)$  is  $L^1$  the first and the last integrals are  $o(1)$  as  $\Omega \rightarrow \infty$ . Because  $F(s)$  vanishes as  $|s| \rightarrow \infty$  on  $\text{Re}(s) \geq -\sigma_0$  and  $\sigma_1$  is arbitrary, the third integral  $\Gamma_3$  is also  $o(1)$  for  $t < 0$ . Denote the second integral as  $I_2$ .

$$I_2 \ll \max_{\sigma_0} |F(s)| \int_{\sigma_0}^{\sigma_1} e^{\omega t} d\omega / (2\pi) = \max_{\sigma_0} |F(s)| (e^{\sigma_1 t} - e^{\sigma_0 t}) / 2\pi t. \quad (B17)$$

For  $\sigma_1 > 0$  and with  $\sigma_0$  and  $t > 0$  fixed, we have  $\max |F(s)| / t \rightarrow o(1)$ .

Therefore,  $f(t) \rightarrow o(1)$  as  $\Omega \rightarrow \infty$  for  $t < 0$ .

(F) The result follows by the Riemann-Lebesgue Lemma [App. A].

**Theorem B5.** Under the hypotheses of Theorem B4 with the additional assumption (iv)  $F(s)$  is analytic on the line  $\text{Re}(s) = -\sigma_0$ , then the Laplace Transform of  $f(t)$  converges at each  $s$  with  $\sigma \geq \sigma_0$  to  $F(s)$ .

**Proof.** Because  $F(s)$  is analytic on  $\text{Re}(s) = -\sigma_0$ , Dini's Criterion certainly holds. Thus, as in the proof of Theorem B2 with the roles of  $f(t)$  and  $F(s)$  interchanged, the Laplace Transform of  $f(t)$  exist and equals  $F(s)$  at each  $s$  on the vertical line  $\text{Re}(s) = -\sigma_0$ . For several reasons, e.g. (B4), this Laplace Transform also converges on  $\text{Re}(s) \geq \sigma_0$  to a function  $F_1(s)$  analytic on  $\text{Re}(s) > \sigma_0$  that agrees with  $F(s)$  on  $\text{Re}(s) = -\sigma_0$ .

By employing integration by parts,  $F_1(s)$  can be shown to be continuous at each point of the line  $\text{Re}(s) = -\sigma_0$ , at the very least when approaches from the right are limited to sectors with angle opening less than  $\pi$ . Then the difference  $G(s) = F(s) - F_1(s)$  is analytic on the open RHP  $\text{Re}(s) > \sigma_0$ , and sectorially continuous at each point of the line



$\operatorname{Re}(s)=\sigma_0$ . The author is indebted to Dr. Wade Ramey for the remainder of the proof.

Let  $E_n = \{\omega: |G(\sigma+j\omega)| \leq n, \sigma \leq \sigma_0 \leq \sigma_0+1\}$ . These sets  $E_n$  are closed and hence by the Baire Category Theorem [Rudin 1973], some  $E_n$  must contain an interval. But then  $G(s)$  is uniformly bounded on a rectangle, one of whose sides coincide with the vertical line  $\operatorname{Re}(s)=\sigma_0$ . By  $H^\infty$  theory [Rudin 1973], since  $G(s)$  is continuous along horizontal lines with limit zero on an open portion of the boundary,  $G(s)$  is identically zero within the rectangle giving that  $F_1(s)=F(s)$  on  $\operatorname{Re}(s)=\sigma_0$ .



## REFERENCES

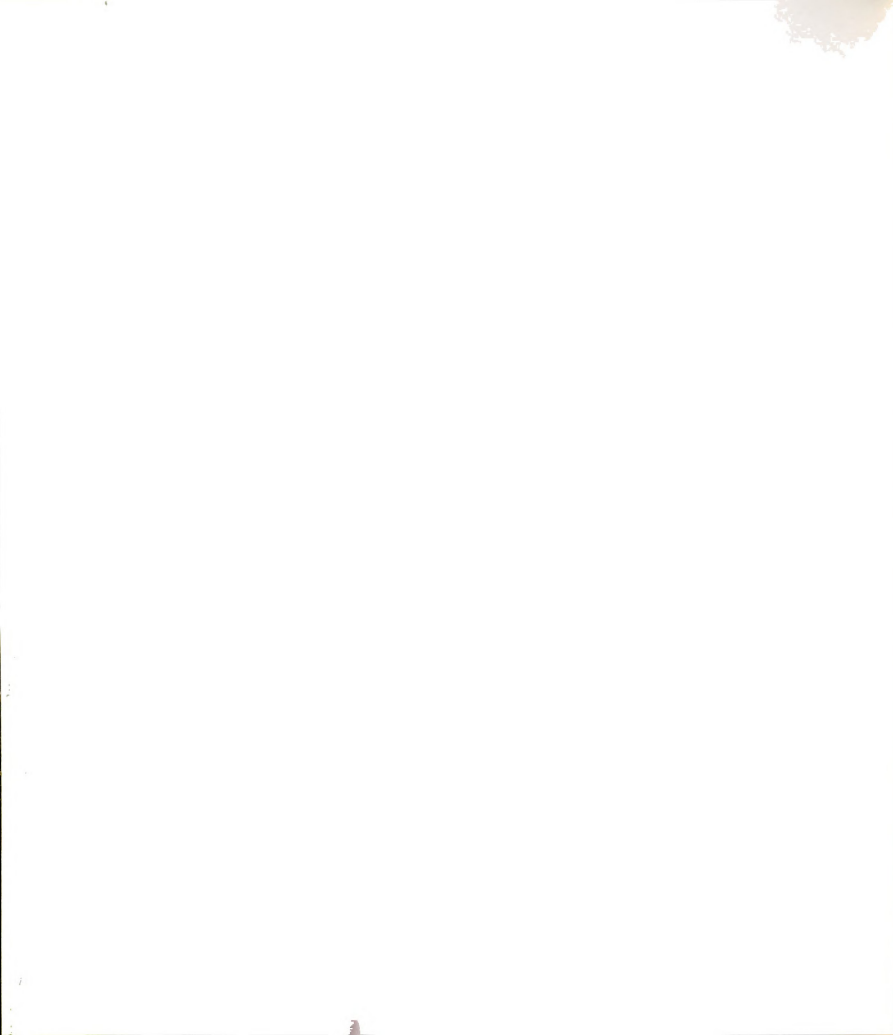


## REFERENCES

- Aubrun, J.N., (1980). "Theory of the Control of Structures by Low-Authority Controllers", *AIAA J. of Guidance, Control, and Dynamics*, 3, pp. 444-451.
- Aubrun, J.N., and Ratner, M.J., (1984). "Structural Control for a Circular Plate", *AIAA J. of Guidance, Control, and Dynamics*, 8, pp. 535-545.
- Balas, M.J., (1978). "Feedback Control of Flexible Systems", *IEEE Transactions on Automatic Control*, AC-23, pp. 673-679.
- Balas, M.J., (1979). "Direct Velocity Feedback Control of Large Space Structures", *AIAA J. of Guidance, Control, and Dynamics*, 2, pp. 252-253.
- Balas, M.J., (1982). "Trends in Large Space Structure Control Theory: Fondest Hopes, Wildest Dreams", *IEEE Transactions on Automatic Control*, AC-27, pp. 15-33.
- Balas, M.J., (1983). "The Galerkin Method for Feedback Control of Linear Distributed Parameter Systems", *J. Mathematical Analysis and Applications*, 91, pp. 527-546.
- Banks, S., (1983). *State-Space and Frequency Domain Methods in the Control of Distributed Parameter Systems*, IEE, Peter Peregrinus Ltd.
- Barker, D.S., and Jacquot, R.G., (1986). "Spillover Minimization in the Control of Self-Adjoint Distributed Parameter Systems", *The J. of the Astronautical Sciences*, 34, pp. 133-146.
- Baldry, R.D., and Breakwell, J.A., (1983). "A Hardware Demonstration of Control for a Flexible Offset-Feed Antenna", *The J. of the Astronautical Sciences*, XXXI, pp. 455-470.



- Benhabib, R.J., Iwens, R.P., and Jackson, R.L., (1983). "Stability of Distributed Control for Large Flexible Structures Using Positivity Concept", *Proceedings of the AIAA Guidance and Control Conference*, pp. 540-548.
- Bernstein, D.S, and Hyland, D.C., (1986). "The Optimal Projection Equations for Finite-Dimensional Fixed-Order Dynamic Compensators of Infinite-Dimensional Systems", *SIAM J. Control and Optimization*, 24, pp. 122-151.
- Bontsema, J., and Curtain, R.F., (1986). "Comparision of Robustness of some Controllers on a Flexible Beam", *Proceedings of the Conference on Decision and Control*, pp. 165-166.
- Book, W.J., and Majette, M., (1985). "Controller Design for Flexible, Distributed Parameter Mechanical Arm Via Combined State Space and Frequency Domain Techniques", *ASME J. of Dynamic Systems, Measurement, and Control*, 105, pp. 245-254.
- Breakwell, J.A., and Chambers, G.J., (1983). "The Toysat Structural Control Experiment", *The J. of the Astronautical Sciences*, XXXI, pp. 441-454.
- Burke, S.E. and Hubbard, J.E., Jr., (1987). "Active Vibration Control of a Simply Supported Beam Using a Spatially Distributed Actuator", *IEEE Control Systems Magazine*, 8, pp. 25-30.
- Calico, R.A., Jr., and Janiszewski, A.M., (1979). "Control of Flexible Satellite Via Elimination of Observation Spillover", *Proceedings of the 1st VPI&AIAA Symposium on Dynamics and Control of Large Structures*, pp. 15-33.
- Callier, F.M., and Desoer, C.A., (1972). "A Graphical Test for Checking the Stability of a Linear Time-Invariant Feedback System", *IEEE Transactions on Automatic Control*, AC-17, pp. 773-780.
- Callier, F.M., and Winkin, J., (1986). "Distributed System Transfer



- Functions of Exponential Order", *International J. of Control*, 43, pp. 1353-1373.
- Cannon, R.H., Jr., and Schmitz, E., (1984a). "Precise Control of Flexible Manipulators", *Robotics Research*, pp. 841-861.
- Cannon, R.H., and Rosenthal, D.E., (1984b). "Experiments in Control of Flexible Structures with Noncollocated Sensors and Actuators", *AIAA J. of Guidance, Control, and Dynamics*, 7, pp. 546-553.
- Chait, Y., Radcliffe, C.J., and MacCluer, C.R., (1988a). "Frequency Domain Stability Criterion for Vibration Control of the Bernoulli-Euler Beam", *ASME J. of Dynamic Systems, Measurement, and Control*, to appear.
- Chait, Y., Radcliffe, C.J., and MacCluer, C.R., (1988b). "A Nyquist Stability Criterion for Distributed Parameter Systems", *IEEE Transactions on Automatic Control*, to appear.
- Chait, Y., Radcliffe, C.J., and MacCluer, C.R., (1988c). "Control of Distributed-Parameter Systems Using Truncated Models -- Guaranteed Closed-Loop Stability and Frequency Response Design", ASME Winter Annual Meeting, to be presented.
- Chait, Y., and Radcliffe, C.J., (1988d). "Control of Flexible Structures with Spillover using an Augmented Observer", *AIAA J. of Guidance, Control, and Dynamics*, to appear.
- Chait, Y., Miklavcic, M, Radcliffe, C.J., and MacCluer, C.R., (1988e). "A Truncated Model for Control of a Flexible Robot Arm", *Proceedings of the 19th annual Pittsburgh Conference on Modeling & Simulation*, to be presented.
- Chen, G., and Russell, D.L., (1982). "A Mathematical Model for Linear Elastic Systems with Structural Damping", *Quarterly of Applied Mathematics*, 39, pp. 433-454.
- Chen M.J., and Desoer C.A. (1982). "Necessary and Sufficient Condition

- for Robust Stability of Linear Distributed Feedback Systems", *International J. of Control*, 35, pp. 255-267.
- Curtain, R.F., and Pritchard, A.J., (1978). *Infinite-Dimensional Linear Control Theory*, Lecture Notes in Control, Springer-Verlag.
- Curtain, R.F., (1985). "Pole Assignment for Distributed Systems by Finite-Dimensional Control", *Automatica*, 21, pp. 57-67.
- Curtain, R.F., and Glover, K., (1986a). "Robust Stabilization of Infinite Dimensional Systems by Finite Dimensional Controllers", *Systems & Control Letters*, 7, pp. 41-47.
- Curtain, R.F., and Zwart, H.J., (1986b). " $L_\infty$  - Approximations of Nonrational Transfer Function: An Example", *Proceedings of the Conference on Decision and Control*, pp. 167-168.
- Desoer, C.A., (1965). "A General Formulation of the Nyquist Criterion", *IEEE Transaction on Circuit Theory*, CT-15, pp. 230-234.
- Desoer, C.A., and Wu, M., (1968). "Stability of Linear Time-Invariant Systems", *IEEE Transactions on Circuit Theory*, CT-15, pp. 245- 250.
- Desoer, C.A., and Vidyasagar, M., (1975). *Feedback Systems: Input-Output Properties*, Academic Press, Ch. IV Sec 4-5.
- Desoer, C.A., and Callier, F.M., (1978). "An Algebra of Transfer Functions for Linear Time-Invariant Systems", *IEEE Transactions on Circuits and Systems*, CAS-25, pp. 651-662.
- Desoer, C.A., and Wang, Y., (1980). "On the Generalized Nyquist Stability Criterion", *IEEE Transactions on Automatic Control*, AC-25, pp. 187-196.
- Doetsch, G., (1962). *Guide to the Applications of Laplace Transforms*, D. Van Nostrand Co.
- Doyle, J.C., and Stein, G., (1981). "Multivariable Feedback Design: Concepts for a Classical/Modern Synthesis", *IEEE Transactions on Automatic Control*, AC-26, pp. 4-16.



- Franke, D., (1985). "Application of Extended Gershgorin Theorems to Certain Distributed-Parameter Control Problems", *Proceedings of the 24th Conference on Decision and Control*, pp. 1151-1156.
- Foias, C., and Tannenbaum, A., (1988). "Optimal Sensitivity Theory for Multivariable Distributed Plants", *International J. of Control*, 47, pp. 985-992.
- Gibson, J.S., (1980). "A Note on Stabilization of Infinite Dimensional Linear Oscillator by Compact Linear Feedback", *SIAM J. Control and Optimization*, 18, pp. 311-316.
- Gibson, J.S., (1981). "An Analysis of Optimal Modal Regulation: Convergence and Stability", *SIAM J. Control and Optimization*, 19, pp. 686-706.
- Glover, K., (1986). "Robust Stabilization of Linear Multivariable Systems: Relations to Approximations", *International J. of Control*, 43, pp. 741-766.
- Hablani, H.B., (1982). "Constrained and Unconstrained Modes: Some Modeling Aspects of Flexible Aircraft", *J. of Guidance, Control, and Dynamics*, 5, pp. 164-173.
- Hallauer, Wm. L., Skidmore, G.R., and Gehling, R. N., (1985). "Modal-Space Active Damping of a Plane Grid: Experiment and Theory", *AIAA J. of Guidance, Control, and Dynamics*, 8, pp. 366-373.
- Halmos, P., (1950). *Measure Theory*, D. Van Nostrand Co.
- Hastings, G.G., and Book, W.J., (1987). "A Linear Dynamic Model for Flexible Robotic Manipulators", *IEEE Control Systems Magazine*, 8, p. 61-64.
- Hille, E., (1959). *Analytic Function Theory*, Vol. I, Ginn and Company.
- Hu, A., Skelton, E.E., and Yang, T.Y., (1987). "Modeling and Control of Beam-like Structures", *J. of Sound and Vibration*, 117, pp. 475-496.
- Hughes, P.C., (1980). "Modal Identities for Elastic Bodies With

- Application to Vehicle Dynamics and Control", *J. of Applied Mechanics*, 47, pp. 177-184.
- Hughes, P.C., (1987). "Space Structure Vibration Modes: How Many Exist? Which Are Important?", *IEEE Control Systems Magazine*, 8, pp. 22-28.
- Jain, A., and Balas, M.J., (1987). "A New Approach to the Design of Low Order Compensators for Distributed Parameter Systems", *Proceedings of the American Control Conference*, pp. 2132-2134.
- Johnson, T.L., (1983). "Progress in Modelling and Control of Flexible Spacecraft", *The Franklin Institute*, 315, pp. 495-520.
- Joshi, S.M., and Groom, N.J., (1980). "Optimal Member Damper Controller Design for Large Space Structures", *AIAA J. of Guidance, Control, and Dynamics*, 3, pp. 378-380.
- Juang, J.N., Horta, L.G., and Robertshaw, H.H., (1986). "A Slewing Control Experiment for Flexible Structures", *AIAA J. of Guidance, Control, and Dynamics*, 9, pp. 599-607.
- Kanoh, H., Tzafestas, S., Lee, H.G., and Kalat, J., (1985). "Modeling and Control of Flexible Robot Arms", *Proceedings of the 25th Conference on Decision and Control*, pp. 1866-1870.
- Khatri, H.C., (1970). "Frequency Domain Stability Criteria for Distributed Parameter Systems", *ASME J. of Basic Engineering*, 92, pp. 377-384.
- Klein, R.G., and Nachtigal, C.L., (1975a). "A Theoretical Basis for the Active Control of a Boring Bar Operation", *J. of Dynamic Systems, Measurement, and Control*, 97, pp. 172-178.
- Klein, R.G., and Nachtigal, C.L., (1975b). "The Application of Active Control to Improve Boring Bar Performance", *ASME J. of Dynamic Systems, Measurement, and Control*, 97, pp. 172-178.
- Komine, I., Takahashi, I., and Ishiro, S., (1987). "Heat Control for Electric Resistance Welding in Steel Pipe Production", *IEEE Control*



- Systems Magazine*, 8, pp. 10-14.
- Lausterer, G.K., and Ray, W.H., (1979). "Distributed Parameter State Estimation and Optimal Feedback Control -- An Experimental Study in Two Dimensions", *IEEE Transaction on Automatic Control*, AC-24, pp. 179-190.
- Leipholtz, H.H.E., (1979). *Structural Control*, North-Holland SM Publications.
- Leipholtz, H.H.E., (1984). "On the Spillover Effect in the Control of Continuous Elastic Systems", *Mechanics Research Communications*, 11(3), pp. 217-226.
- Leipholtz, H.H.E., and Abdel-Rohman, M., (1986). *Control of Structures*, Martinus Nijhoff Publishers.
- Leonhard, A., (1953). "Determination of Transient Response from Frequency Response", *Frequency Response*, edited by Oldenburger, R., The Macmillan Co.
- Longman, R.W., (1979). "Annihilation or Suppression of Control and Observation Spillover in the Optimal Shape Control of Flexible Spacecraft", *The J. of Astronautical Sciences*, XXVII, pp. 381-399.
- MacCluer, C.R., (1988). "Stability from an Operation Viewpoint", *IEEE Transactions on Automatic Control*, 23, pp. 458-460.
- MacFarlane, A.G.J., and Postlethwaite, I., (1977). "The Generalized Nyquist Stability Criterion and Multivariable Root Loci", *International J. of Control*, 25, pp. 81-127.
- MacFarlane A.G.J, and Postlethwaite, I., (1978). "Extended Principle of the Argument", *International J. of Control*, 27, pp. 49-55.
- Mashkovskii, A.G., and Potapenko, L.S., (1983). "Approximation of Operators and Synthesis of Modal Control of Systems with Distributed Parameters", *Kibernetika i Vychislitel'naya Tekhnika*, pp. 146-154.
- Meirovitch, L., (1967). *Analytical Methods in Vibrations*,

The Macmillan Co.

- Meirovitch, L., and Baruh, H., (1983). "On the Problem of Observation Spillover in Self-Adjoint Distributed-Parameter Systems", *J. of Optimization Theory and Applications*, 39, pp. 269-290.
- Nett, C.N., Jacobson, C.A., and Balas, M.J., (1983). "Fractional Representation Theory: Robustness Results with Applications to Finite Dimensional Control of a Class of Linear Distributed Systems", *Proceedings of the Conference on Decision and Control*, pp. 268-280.
- Nyquist, H., (1932). "Regeneration Theory", *Bell System Technical J.*, 11, pp. 126-147.
- Nurre, G.S., Ryan, R.S., Scofield, H.N., and Sims J.L., (1984). "Dynamics and Control of Large Space Structures", *AIAA J. of Guidance, Control, and Dynamics*, 7, pp. 514-526.
- Ogata, K., (1970). *Modern Control Engineering*, Prentice-Hall.
- Ozguner, U., and Yurkovich, S., (1987). "Active Vibration of the OSU Flexible Beam", *Proceedings of the American Control Conference*, pp. 970-975.
- Papoulis, A., (1962). *The Fourier Integral and its Applications*, McGraw-Hill Co, p. 214.
- Pohjolainen, S.A., (1982). "Robust Multivariable PI-Controller for Infinite Dimensional Systems", *IEEE Transactions on Automatic Control*, AC-27, pp. 17-30.
- Radcliffe, C.J., and Mote, C.D. Jr., (1983). "Identification and Control of Rotating Disk Vibration", *J. of Dynamic Systems, Measurement, and Control*, 105, pp. 39-45.
- Rakhsha, K., and Goldenberg A.A., (1985). "Dynamics of a single link Flexible Robot", *Proceedings of the IEEE International Conference on Robotics and Automation*, pp. 984-989.



- Ray, W.H., (1978). "Some Recent Applications of Distributed Parameter Systems Theory--A Survey", *Automatica*, 14, pp. 281-287.
- Rudin, W., (1973). *Functional Analysis*, McGraw-Hill.
- Russell, D.L., (1969). "Linear Stabilization of the Linear Oscillator in Hilbert Space", *J. of Mathematical Analysis and Applications*, 25, pp. 663-657.
- Russell, D.L., (1979). *Mathematics of Finite-Dimensional Control Systems - Theory and Design*, Marcel Dekker.
- Sakawa, Y., (1983). "Feedback Stabilization of Linear Diffusion systems", *SIAM J. Control and Optimization*, 21, pp. 667-676.
- Schaechter, D.B., (1982). "Hardware Demonstration of Flexible Beam Control", *AIAA J. of Guidance, Control, and Dynamics*, 5, pp. 48-53.
- Schafer, B.E., and Holzach, H., (1985). "Experimental Research on Flexible Beam Modal Control", *AIAA J. of Guidance, Control, and Dynamics*, 8, pp. 597-604.
- Schumacher, J.M., (1983). "A Direct Approach to Compensator Design for Distributed Parameter Systems", *SIAM J. Control and Optimization*, 21, pp. 823-836.
- Sesak, J.R., Likins, P., and Coradetti, T., (1979). "Flexible Spacecraft Control by Model Error Sensitivity Supression", *The J. of the Astronautical Sciences*, XXVII, pp. 131-156.
- Simon, J.D., and Mitter, S.K., (1968). "A Theory of Modal Control", *Information and Control*, 13, pp. 316-353.
- Skelton, R.E., and Likins P.W., (1978). "Orthogonal Filters for Model Error Compensation in the Control of Nonrigid Spacecraft", *AIAA J. of Guidance, Control, and Dynamics*, 1, pp. 41-49.
- Sundararajan, N., and Montgomery, R.C., (1984). "Adaptive Control of a Flexible Beam Using Least Square Lattice Filters", *IEEE Transactions on Aerospace and Electronic Systems*, AES-20, pp. 541-546.

- Takahashi, Y., Rabins, M.J., and Auslander, D.M., (1970). *Control and Dynamic Systems*, Addison-Wesley Publishing Co.
- Tolstov, G.P., (1962). *Fourier Series*, Prentice-Hall.
- Trench, W.F., (1978). *Advanced Calculus*, Harper & Row.
- Triggiani, R., (1975). "On the Stabilizability Problem in Banach Space", *J. of Mathematical Analysis and Applications*, 52, pp. 383-403.
- Ulsoy, A.G., (1984). "Vibration Control in Rotating or Translating Elastic Systems", *ASME J. of Dynamic Systems, Measurement, and Control*, 106, pp. 6-14.
- Vidyasagar, M., (1972). "Input-Output Stability of a Broad Class of Linear Time-Invariant Multivariable Systems", *SIAM J. Control*, 10, pp. 203-209.
- Vidyasagar, M., (1975). "Copriime Factorization and Stability of Multivariable Distributed Feedback Systems", *SIAM J. Control*, 13, pp. 1144-1155.
- Vidyasagar, M., (1985). *Control System Synthesis*, The MIT Press.
- Vidyasagar, M., and Morris, K.A., (1987). "An Analysis of Euler-Bernoulli Beams From the Standpoint of Controller Design", *Modeling and Control of Robotic Manipulators and Manufacturing Processes*, ASME Publication, DSC Vol. 6, pp. 297-305.
- Vidyasagar, M., Bertschmann, R.K., and Sallaberger, C.S., (1988). "Some Simplifications of the Graphical Nyquist Criterion", *IEEE Transactions in Automatic Control*, AC-33, pp. 301-305.
- Wie, B., (1981). *On the Modeling and Control of Flexible Space Structures*, Ph.D. Thesis, Stanford University.





MICHIGAN STATE UNIV. LIBRARIES



31293000541098